

ARR Aug. 1942

NATIONAL ADVISORY COMMITTEE FOR AERONAUTICS

# WARTIME REPORT

ORIGINALLY ISSUED

August 1942 as  
Advance Restricted Report

THE STRENGTH OF PLANE WEB SYSTEMS IN

INCOMPLETE DIAGONAL TENSION

By Paul Kuhm and Patrick T. Chiarito

Langley Memorial Aeronautical Laboratory  
Langley Field, Va.

The NACA logo is a stylized wing shape with the letters "NACA" in a bold, sans-serif font. The wings are represented by two sets of parallel lines that taper towards the center, creating a sense of motion and aerodynamics. The logo is centered on the page and is the largest graphic element.

## NACA

WASHINGTON

NACA WARTIME REPORTS are reprints of papers originally issued to provide rapid distribution of advance research results to an authorized group requiring them for the war effort. They were previously held under a security status but are now unclassified. Some of these reports were not technically edited. All have been reproduced without change in order to expedite general distribution.



# NATIONAL ADVISORY COMMITTEE FOR AERONAUTICS

## ADVANCE RESTRICTED REPORT

### THE STRENGTH OF PLANE WEB SYSTEMS IN INCOMPLETE DIAGONAL TENSION

By Paul Kuhn and Patrick T. Chiarito

#### SUMMARY

Two series of diagonal-tension beams with double uprights were tested to destruction while strain measurements were being made at a large number of points. The results indicated that the previously published method of stress analysis is somewhat conservative in a certain range; the discrepancy between theory and tests was reduced by dropping a simplifying assumption, and a set of correspondingly revised formulas for stress analysis is given in a form suitable for ready reference.

On the basis of the revised formulas, more than 100 tests made by five manufacturers were analyzed. Most of these tests were made on beams with single uprights. An empirical formula for the failing stress in single uprights was derived from the tests.

An appendix presents the results of systematic calculations on structural efficiency. The graphs of the appendix may be used to obtain first approximations of sizes for design purposes.

#### INTRODUCTION

A semiempirical theory for the action of shear webs in incomplete diagonal tension has been developed in reference 1. The empirical coefficients for this theory were chiefly obtained by strain-gage tests at low stresses. In order to check the validity of these coefficients at high stresses, a new investigation was started in which a number of beams were tested to failure while the strains were being measured with electrical strain gages. All the tests were made on webs with double uprights. In-

formation on the failure of single uprights was obtained by analyzing the results of tests made by five manufacturers. These tests were made available to the NACA by the joint action of the Army, the Navy, and the Civil Aeronautics Authority in a general effort to effect coordination between existing structural data and theories. The manufacturers' tests also yielded some information on web failures and rivet failures.

The paper is divided into two parts. The first part deals with the experimental investigation carried out by the NACA. The second part is of an analytical nature and is divided into two sections. The first section gives the formulas used for stress analysis in a form suitable for ready reference. The second section discusses the amount of experimental evidence available on specific items, the scatter indicated by the test data, and other pertinent information that may be useful in judging the reliance to be placed on any given formula. An appendix discusses the question of structural efficiency of the web system on the basis of the new formulas for stress analysis. The graphs given may be used as aids in obtaining the proportions for a balanced design.

Attention is called to the fact that some symbols used in this report have a slightly different meaning than in reference 1. The changes were made to permit simplification of a number of formulas.

## SYMBOLS

$A_U$	actual cross-sectional area of upright, square inches
$A_{U_e}$	effective cross-sectional area of upright, square inches
$C_R$	rivet factor $\left(1 - \frac{\text{rivet diameter}}{\text{rivet pitch}}\right)$
$C_1, C_2$	stress factors
$E$	modulus of elasticity, kips per square inch
$G$	shear modulus, kips per square inch

---

$G_e$	effective shear modulus, taking into account diagonal-tension effects
$\bar{G}_e$	effective shear modulus, taking into account diagonal-tension effects and effects of exceeding the proportional limit of the material
$L_e$	effective column length of upright, inches
$P$	applied load, kips
$P_U$	internal force in upright, kips
$P_{ult}$	ultimate applied load, kips
$S$	transverse shear force in web, kips
$V$	volume of material (web and uprights) per inch run, square inches
$d$	spacing of uprights, inches
$h$	depth of beam, back of top flange to back of bottom flange, inches
$h_c$	effective depth of beam, centroid of top flange to centroid of bottom flange, inches
$h_R$	depth of beam, centroid of rivets in top flange to centroid of rivets in bottom flange, inches
$h_U$	length of upright, centroid of attachment rivets in top flange to centroid of attachment rivets in bottom flange, inches
$k$	diagonal-tension factor
$t$	thickness of web, inches
$t_U$	thickness of uprights, inches
$\alpha$	angle between axis of beam and direction of diagonal tension
$\epsilon$	strain in web parallel to axis of diagonal tension

$\epsilon_x$	strain in flange caused by diagonal tension
$\epsilon_y$	strain in upright caused by diagonal tension
$\rho$	radius of gyration of cross section of upright with respect to centroidal axis parallel to web, inches
$\sigma_U$	compressive stress in upright caused by diagonal tension, kips per square inch
$\tau$	nominal shear stress in web, kips per square inch. In most cases, this stress may be computed by the approximate formula $\tau = S/h_w t$
$\tau_{cr}$	critical shear stress, kips per square inch
$\tau_{eq}$	equivalent shear stress, kips per square inch
$wd$	parameter of flange flexibility

## I. EXPERIMENTAL INVESTIGATION

### Test Objects and Procedures

Test specimens.- The test specimens consisted of 13 beams in two series with nominal depths of 40 inches and 25 inches. The detailed dimensions of the beams are given in table I. The webs and the uprights were of 24S-T aluminum alloy with the exception of the web on beam 25-3, which was of 17S-T alloy. The flanges of the 40-inch beams were of steel. The flanges of the 25-inch beams were of 24S-T aluminum alloy. Figure 1 gives the general dimensions of the beams and figure 2 shows the cross sections of the uprights.

Test procedure.- The beams were attached to a heavy steel structure by steel angles. When the maximum test loads were larger than 8 kips, the test loads were applied to the beams by a portable hydraulic jack of 100-kips capacity. This portable jack is equipped with a load-indicating system of the hydraulic type used in testing machines. For loads less than 8 kips, a hand-operated hydraulic jack was used, and the load was measured with a platform scale of 12 kips capacity. A typical set-up for a 25-inch beam is shown in figure 3.

Most strain measurements were made with electrical strain gages of the wire-resistance type fabricated by the NACA. Gages were always used in pairs on opposite sides of the beams to eliminate the effects of local bending stresses. For purposes of strain measurements, end effects were assumed to exist over a lengthwise distance equal to half the depth of the beam from the root and from the tip. Strain measurements were usually taken on all of the uprights and in all of the web panels not subjected to the end effects. The test results shown in the figures are group averages obtained by averaging the results of all gages contained in the same lengthwise group. The number of strain gages used for one test varied from 32 to 70; the smallest number were used with an upright spacing equal to the depth of the beam.

Deflections of the beams were measured by the method shown schematically in figure 4. A light truss holding dial gages reading to 0.001 inch was fastened to the beam by means of a vertical arm. This arm was securely fastened to the upper and the lower flange of the beam at the station where the inboard web reinforcement ended. The outermost dial was located at the station where the outboard web reinforcement began. The deflection measurements were thus confined to the region where the web was of single thickness, and the reference line was the tangent to the elastic line of the beam at the inboard end of this region.

In order to prevent failure of the beams by twisting, lateral support was provided in the form of parallel-motion links. These links consisted of two angles each and were held at the far ends by a space trusswork bolted to the backstop. The tip of this trusswork is visible in figure 3 just beyond the tip of the beam. The links may be seen in figure 5.

Deflections of the uprights normal to the plane of the web were measured on some beams by dial gages, as shown in figure 6. These measurements were abandoned because the deflections were practically zero in the load range where it was considered safe to leave the gages in place.

The 45° triangle prominent in figure 6 was used to measure the elongation of a 45° line. Microscopes equipped with filar micrometers were clamped to the angle and served as measuring instruments. The measurements were intended

chiefly to check for the existence of permanent elongation in the web. They were abandoned after a few tests because it was found that permanent set began later than anticipated and that the predictions of upright failures were unreliable and unconservative. The unexpected occurrence of upright failure jeopardized the safety of the equipment.

Failure of the uprights by forced twisting is shown in figure 7. This type of failure is typical of thin uprights.

Accuracy of measurements.— The errors of the load measurements were not more than one-half of 1 percent. Web thicknesses were measured on a large number of stations; the average thickness can probably be relied on to  $\pm 0.0003$  inch. The cross-sectional areas of the uprights and of the flanges were determined by weighing, except for the steel flanges used on beam 40-1 and beam 40-2, which were determined by measurement. Cross-sectional areas for aluminum-alloy sections determined by weighing are probably accurate to  $\pm 1$  percent; the errors in the cross-sectional areas of the steel flanges are probably larger, particularly when determined by measurements, but it is not possible to give quantitative estimates. The accuracy of the strain measurements is estimated to  $\pm 4$  percent.

### Test Results

Stresses in webs.— The strain measurements on the webs were taken at angles of  $45^\circ$  with the beam axes. The observed strains were multiplied by the factor  $E$  to obtain stress values; the resulting stresses were, of course, nominal because the state of stress was actually two-dimensional. When the stresses exceeded the proportional limit, the stress-strain curve of the material was used to convert the measured strains into stresses. Individual stress-strain curves were taken only for the webs expected to fail before failure of the uprights took place; an average stress-strain curve was used to convert the strain readings on the other webs into stresses. The resulting experimental stress values are shown in figure 8.

The calculated stresses shown in figure 8 were obtained as follows:

The theory of incomplete diagonal tension developed in reference 1 assumes that the stress in the web can be described by superposing the effects of a diagonal-tension load  $kS$  and a shear load  $(1 - k)S$ . If the angle  $\alpha$  of the diagonal tension is assumed to be  $45^\circ$ , the nominal stress along a  $45^\circ$  line is

$$\begin{aligned} \bar{\sigma}_c &= \bar{\sigma} \left[ \frac{2\tau k}{\bar{\sigma}} + \frac{\tau(1 - k)(1 + \mu)}{\bar{\sigma}} \right] \\ &= \tau \left[ 1 + \mu + k(1 - \mu) \right] \end{aligned} \quad (1)$$

The value of Poisson's ratio  $\mu$  was taken as 0.30. The stress given by formula (1) is an average stress. The maximum stress is given by the formula

$$\bar{\sigma}_c = \tau \left[ 1 + \mu + k(1 - \mu) \right] (1 + kC_2) \quad (1a)$$

where  $C_2$  is a factor of stress concentration caused by flexibility of the flanges; this factor will be discussed later.

The stress given by formula (1) is plotted in figure 8 as a dashed line, the stress given by formula (1a) as a solid line. The stresses calculated by formula (1a) should be compared with the stresses measured on diagonal-tension lines passing through the joints between uprights and flanges. No correction was made to allow for the fact that the angle  $\alpha$  was not exactly equal to  $45^\circ$ . The error involved is a cosine error and was about  $1\frac{1}{2}$  percent in the worst case.

The agreement between experimental and calculated values is satisfactory on the 40-inch beams, excepting the stresses in beam 40-1 at loads above 15 kips. No definite cause has been established for the discrepancy, but two factors may have a bearing on the subject: The beam was loaded a number of times to 15 kips, and the strain gages used were not suitable for use on buckled sheet. A different type of gage was used in all the other tests.



On the 25-inch beams the experimental stresses show a tendency to be somewhat low. It is believed that this discrepancy can be ascribed to portal-frame action (fig. 9). This explanation is supported by figure 3, which shows beam 25-1 carrying a load of 1570 pounds or 23 percent of the ultimate load after the web had been completely ruptured from flange to flange. The reverse curvature of the flanges typical of portal-frame action is very evident in figure 3.

If it is assumed, as a first approximation, that the shear deformation of the web and the portal-frame action do not influence each other, the shear  $S'$  that is carried by the web is related to the total shear  $S$  by the expression

$$\frac{S'}{S} = \frac{1}{1 + \frac{24EI}{L_p^3 h t G_s}} \quad (2)$$

where  $EI$  is the bending stiffness of one flange and  $L_p$  is the effective "height" of the portal frame. Values of  $S'/S$  are given in table II; these values are based on the assumption that  $L_p$  may be taken as the length of web of single thickness (fig. 9), that is, the end bays having triple thickness are considered as rigid. Inspection of figure 8 and of the values of  $S'/S$  in table II indicates that the differences between experimental and calculated stresses would be reduced if the portal-frame action were taken into account; only on beam 25-4 would there be a larger difference of an unconservative nature. In order to avoid confusion on the figure, no corrected calculated curves are shown.

Stresses in uprights.— On the first 40-inch beam, a detailed survey of stresses in the uprights was made with Tuckerman strain gages to study the effect that was termed "gusset effect" in reference 1. The results of the strain survey are shown in figure 10. It will be seen that the gusset effect is very pronounced on the tension side (bottom side) of the beam. On the compression side, however, no gusset effect can definitely be said to exist except near the tip; the average of all uprights shows a gusset effect only at the tension side of the beam.

The measurements made with electrical strain gages on the other beams are summarized in figure 11. No stresses on individual uprights are shown in figure 11, but the averages shown are sufficient to indicate that the evidence concerning the gusset effect is conflicting. On the 25-inch beams with 0.011- and 0.016-inch webs, there is practically no evidence of gusset effect. It would therefore seem advisable to drop the use of the gusset factor as a refinement not warranted by the present state of knowledge.

Figure 12 shows the stresses in the uprights plotted against load. For each beam, the stresses shown are those for the most highly stressed station along the uprights in each case. The calculated stresses are generally in good agreement with the maximum experimental values for the 40-inch beams. The only exception is the first 40-inch beam; on this beam, the maximum stresses were higher than the calculated stresses.

On the 25-inch beams, the web was so thin that the condition of pure diagonal tension should have been approached very closely. The upright stresses measured on these beams were therefore expected to be in closer agreement with the theory than the stresses measured on the 40-inch beams. The reverse was true; inspection of figure 12 shows that the measured upright stresses in the 25-inch beams were considerably lower than the calculated stresses. The differences are too large to be explained by portal-frame action, although this action was sufficient to explain most of the differences between observed and calculated web stresses. The theoretical calculation of the angle  $\alpha$  might be thought to be inaccurate; such measurements of  $\alpha$  as were made indicated, however, that  $\alpha$  was slightly above rather than below the calculated value. No explanation for the discrepancy has been found thus far.

The stresses in the uprights constitute the most sensitive criterion for the validity of any theory of incomplete diagonal tension. Figure 12 shows the theory used in this paper to be in very satisfactory agreement with the test results on the 40-inch beams and to be conservative for the 25-inch beams. Webs as thin as those used on the 25-inch beams will seldom be encountered in practice.

Failures of uprights.- On all but beam 25-7, the uprights were rather sturdy ( $t_u/t \approx 3$ ) and failed by column action; a typical failure is shown in figure 5. The ratio of developed strength to predicted strength varied from 0.99 to 1.37 (table II). The uprights on beam 25-7 were designed to fail by forced twisting; the failure is shown in figure 7.

Rivets upright-to-web.- In all except beam 40-1 and beam 25-7, the upright-to-web rivets were designed for the first test to have a strength in double shear approximately equal to the load on the upright at failure (table III). On beam 25-7, the rivet spacing was arbitrarily decreased to make the uprights and the web act as a unit as long as possible in spite of the localized nature of the failure expected, namely, failure by forced twisting.

On beam 40-4a the web was not damaged when the uprights failed. The uprights were removed, straightened and again attached to the beam with the next larger size of rivet. When the uprights were attached, care was taken to shift them around in order to change the relation between the failure pattern of the web and the failure pattern of the uprights. The rivet strength of beam 40-4b was 1.57 times the rivet strength of beam 40-4a, and the load carried was 1.06 times as much as in the first test. The uprights were again removed, straightened and reattached with intermediate rivets added. The rivet strength was now three times the original value, and the beam strength was found to be 1.18 times the original value. (See table II for data.)

Beam deflections.- The comparison between experimental and calculated beam deflections is shown in figure 13. The experimental deflections are considerably lower than the calculated deflections on the 40-inch beams; on the 25-inch beams, the agreement is generally better. The most obvious explanation for the discrepancies would be that the effective shear modulus  $G_e$  obtained from reference 1 is too low, but this obvious explanation does not appear to be the correct one. Plate-girders with thick webs (reference 3) tested in the shear-resistant range gave consistently smaller deflections than the calculations indicated; only a single beam out of 8 gave larger deflections. The difference was about 6 percent for the total deflections and more than twice as much for the shear deflections alone, if the single exception

is excluded. These results indicate that the simple formulas commonly used for computing the bending deflections and shear deflections become conservative when the beams are short and deep, that is, when the length-width ratio is less than about 4 on a cantilever beam. The fact that the discrepancies were larger in the tests on the 40-inch beams than in all other beams may be attributed in part to the fact that the properties of the steel flanges were not so accurately known as the properties of the aluminum-alloy flanges. In addition, an experimental error might have been caused by welding the reference truss to the beam flanges. The welds had a spanwise length of 4 inches, and it is possible that their effective center did not coincide with their geometric center.

Permanent deflections.- Permanent deflections of the beams as indicated by the readings of the dial gages at the tip are tabulated in table IV. For the 0.040-inch webs, the set was only slightly above the accuracy of the measurements at shear stresses up to 10 kips per square inch. In the 0.011- and 0.016-inch webs of the 25-inch beams, a definite permanent deflection was indicated by the dial gages and began at a shear stress of about 12.5 kips per square inch. Visual inspection of the webs on the 40-inch beams showed no obvious wrinkles. On the 25-inch beams, the webs showed pronounced wrinkles of half-moon shape under the ends of the uprights, where the joggles in the uprights left the sheet unsupported and therefore incapable of carrying any compressive stress in the direction of the uprights.

## II. ANALYTICAL INVESTIGATION

### Formulas Used for Stress Analysis

The collection of formulas given in this section was chiefly intended to describe the methods by which the analytical calculations were made. Beyond this purpose, the collection may serve as a guide for stress analysis.

The formulas were either taken directly from reference 1 or are simple additional applications of the basic theory developed in this reference. One important modification of the theory was made by dropping a simplify-

ing assumption made in reference 1; the nature of this modification is discussed under the side heading Design chart for incomplete diagonal tension.

For certain items of design, no formulas have been presented in this section, either because the experimental evidence is inconclusive or because no definite design criterion now exists. These items are discussed in the correlative study of the next section. A careful perusal of the correlative study should precede any attempt to apply the formulas given here.

Effective cross-sectional area of uprights.— Three basic types of upright are shown in figure 14. In type (a), double uprights symmetrical with respect to the web, the effective cross-sectional area of the upright equals the actual area

$$A_{U_e} = A_U$$

In type (b), single uprights on one side of the web, the effective cross-sectional area is defined by the formula (reference 1, equation (23))

$$A_{U_e} = \frac{A_U}{1 + \left(\frac{e}{\rho}\right)^2} \quad (3)$$

where  $e$  is the distance from the web to the centroid of the upright. In type (c), where a transverse member such as a bulkhead is attached by means of a connecting angle, the effective area  $A_{U_e}$  may be assumed to consist of the connecting angle and of an effective width of the transverse member. This type of upright was not used in the present investigation and is included here only for the sake of completeness. No part of the web was included in the area  $A_U$  in any case.

Buckling stress of web.— The buckling shear stress  $\tau_{cr}$  of the web was obtained from figure 15 for simply supported edges. This figure is based on the formula developed by Timoshenko (reference 4). When some or all of the edges of the panels were clamped, the buckling

stress  $\tau_{cr}$  obtained from figure 15 was multiplied by the factor

$$\left(1 + 0.66 \frac{p_c}{p}\right) \quad (4)$$

where  $p$  is the total perimeter of the panel and  $p_c$  the length of the clamped edges. The origin of the factor 1.66 for the condition of all edges fully clamped was discussed in reference 1.

The edge support given by the flanges or the uprights to the sheet was assumed to be the equivalent of fully clamped edges when the sheet was clamped between two angles, provided that each angle was at least three times as thick as the sheet and had flat faces touching the sheet (fig. 16 (a)). The edges of the sheet panel were taken to be the lines where the sheet emerged from underneath the angles (A, fig. 16).

The edge support was assumed to be the equivalent of simply supported edges for the types of upright shown in figure 16 (b), (c), and (d); namely, double uprights consisting of extruded angles having crowned faces touching the sheet, double uprights having a thickness about equal to the thickness of the web, and single uprights. For these 3 types of upright, the edges of the sheet panel were taken to be the rivet lines. The assumptions concerning edge support for upright types (a), (b), and (c) were suggested by the results of strain measurements on uprights. For type (d), the assumptions are justified only in an indirect manner by the final results. A method of relating the edge support to the thickness of the upright and the thickness of the web is given in the appendix.

Design chart for incomplete diagonal tension.— The degree of development of the diagonal-tension field is numerically defined by the diagonal-tension factor  $k$  (reference 1). This factor specifies the portion of the total shear that is carried by diagonal-tension action of the web; it is a function of the ratio  $\Delta U_0/dt$  and the ratio  $\tau/\tau_{cr}$  (reference 1). The numerical values of the factor  $k$  were obtained by inspection from one of the two design charts (fig. 17 or fig. 18). Larger copies of figures 17 and 18 may be obtained on request from the National Advisory Committee for Aeronautics.

The stress in an upright can be calculated by the formula

$$\sigma_U = \frac{k\tau dt}{A_{U_0} + (1 - k)dt} \tan \alpha \quad (5)$$

In reference 1, this formula (equation (13)) was given in a slightly simplified form by omitting the factor  $\tan \alpha$ ; the omission was based on the simplifying assumption that  $\alpha = 45^\circ$ . In order to obtain better agreement with the test data over a wide range of variables, the simplifying assumption was dropped in the present paper, and the values of  $\sigma_U/\tau$  shown in figures 17 and 18 were obtained from the corresponding values of reference 1 by the following process of correction.

The values of  $\sigma_U/\tau$  given in reference 1 were considered as first approximations. According to the theory of pure diagonal tension (reference 2), the angle  $\alpha$  is defined by the equation

$$\tan^2 \alpha = \frac{\epsilon - \epsilon_x}{\epsilon - \epsilon_y} \quad (6)$$

The magnitude of  $\epsilon_x$  is negligible in most practical cases; the magnitudes of  $\epsilon$  and  $\epsilon_y$  were computed by using the first approximations for the stresses as given by reference 1. Formula (6) became under these assumptions,

$$\tan^2 \alpha = \frac{1}{1 + \frac{\sigma_U}{2\tau}} \quad (7)$$

where  $\sigma_U/\tau$  was the first approximation obtained from reference 1. The value of  $\tan \alpha$  was computed by formula (7), and the first approximations of  $\sigma_U/\tau$  obtained from reference 1 were multiplied by  $\tan \alpha$  to obtain the second approximations that are given in figures 17 and 18. The difference between the first approximation and the

second approximation is small when the ratio  $\Delta U_0/dt$  is large but becomes quite large when this ratio is small.

Analysis of web strength.— The stress in the web was expressed as an "equivalent" shear stress defined by the formula

$$\tau_{eq} = \tau(1 + kC_1)(1 + kC_2)/C_R \quad (8)$$

The factor  $C_1$  takes into account the fact that the angle  $\alpha$  is somewhat less than  $45^\circ$  and is given by the expression

$$C_1 = \frac{1}{\sin 2\alpha} - 1 \quad (9)$$

For convenience, the value of  $C_1$  is shown graphically in figure 19. The expression  $(1 + kC_1)$  is simply a formula for straight-line interpolation between the limiting cases of shear and pure diagonal tension. Figure 19 also gives  $\tan \alpha$  as a matter of some interest.

The factor  $C_2$  is shown graphically in figure 20 and was obtained by a simple transformation from the corresponding factor  $C_2'$  given in reference 1. If this corresponding factor is denoted temporarily by  $C_2'$ , then

$$C_2 = \frac{1}{C_2'} - 1 \quad (10)$$

The expression  $(1 + kC_2)$  is again a formula for a straight-line interpolation between the limiting cases of shear and pure diagonal tension. The parameter  $wd$  characterizing the flexibility of the flange is given by the expression

$$wd = 0.89d \sqrt{\frac{t}{(I_T + I_C)h_0}} \quad (11)$$

where  $I_T$  and  $I_C$  are the moments of inertia of the tension flange and of the compression flange; respectively.



Formula (11) is an approximation that is valid as long as the ratio  $I_T/I_C$  does not differ too much from unity.

The allowable web stress was computed by the formula

$$\tau_{eq}(all) = \tau_{ult} - k \left( \tau_{ult} - \frac{1}{2} \sigma_{ult} \right) \quad (12)$$

This formula is equivalent to formula (22) of reference 1. The values of  $\tau_{ult}$  and  $\sigma_{ult}$  were taken from reference 5.

Analysis of uprights. - The stresses in the uprights were computed by the expression

$$\sigma_U = \tau (\sigma_U / \tau) \quad (13)$$

The ratio  $\sigma_U / \tau$  was obtained from one of the two design charts. For double uprights,  $\sigma_U$  represents the average stress in the upright. For single uprights,  $\sigma_U$  represents the maximum stress, that is, the stress in the fibers next to the web.

A visual study of upright failures has led to the conclusion that single uprights of open cross section fail as a result of twisting forced by the folds in the webs upon the uprights. The allowable stress for this type of failure was computed by the empirical formulas

$$\sigma_U(all) = 12.5 \, t_U / t \quad \text{kips per square inch} \quad (14)$$

$$\sigma_U(all) = 10.5 \, t_U / t \quad \text{kips per square inch} \quad (14a)$$

Formula (14) may be considered to represent the average of the test data, and formula (14a) may be considered to represent the lower limit of the test data.

Double uprights of open cross section may fail by forced twisting or they may fail by column failure. Formulas (14) and (14a) were used to check against twisting failure. In order to check against column failure, the effective column length was computed by the formula

$$L_e = \frac{h_U}{\sqrt{1 + k^2(3 - 2d/h)}} \quad (15)$$

for  $(d/h \leq 1.5)$

With this effective length, the slenderness ratio  $L_o/\rho$  was computed and the allowable stress was obtained from the standard column curve for 24S-T material as given in reference 5.

Analysis of rivets web-to-flange.- The load  $R$  per inch acting on the web-to-flange rivets was calculated by the formula

$$R = S(1 + 0.414k)/h_R \quad (16)$$

The allowable rivet loads were taken from reference 5, but a correction was made for the actual drill size used when it was known. The use of this correction is suggested for the analysis of test data but not for ordinary stress analysis.

Analysis of rivets upright-to-flange.- The total force acting on the upright-to-flange rivets is equal to the internal force in the upright, which is

$$P_U = \sigma_U A_U \quad \text{for double uprights} \quad (17a)$$

$$P_U = \sigma_U A_{U_e} \quad \text{for single uprights} \quad (17b)$$

The rivets in double uprights are in double shear; rivets in single uprights are in single shear. Formula (17b) must be modified by an empirical coefficient when used for actual stress analysis. (See section Correlative Study of Manufacturers' Tests and NACA Tests.)

The allowable loads on rivets were taken from reference 5. A correction was made for actual drill size used when it was known. The use of this correction is suggested for the analysis of test data but not for ordinary stress analysis.

Analysis of beam deflections.— The beam deflections were computed by the standard method of adding bending deflections and shear deflections. The moment of inertia used in the computation of the bending deflections was based on the entire gross section; that is, no deductions were made for ineffectiveness of the web or for rivet holes. The shear deflections were computed by the formula

$$\delta = \frac{\tau x}{G_0} \quad (18)$$

where  $x$  is the distance from the reference station to the station being considered. The effective shear modulus  $G_0$  was obtained from figure 24 of reference 1. The correction to  $G_0$  for exceeding the proportional limit was based on the tentative correction curve shown in figure 21, which is based on unpublished tests of 10 shear panels 0.025 and 0.040 inch thick. Within the rather large scatter of the test data, the curve was found to be independent of the degree to which the diagonal tension was developed and may therefore be used for the limiting case of unbuckled sheet when  $G_0 = G$ . The curve then becomes identical with the shear stress-strain curve of the material.

Analysis of alclad webs.— The most satisfactory method of analyzing alclad webs was found to be the following method: The actual web thickness  $t$  was replaced by an effective thickness  $t_0 = 0.9t$ , and the web was then analyzed as though it were made of the basic alloy alone. The effective thickness  $t_0$  was used in all calculations, including the calculation of  $\tau_{cr}$ .

Limitations on use of theory.— On account of the complexity of the problem of incomplete diagonal tension, it has not been possible thus far to explore experimentally the entire range of possible design proportions; limitations must therefore be imposed on the use of the theory. The necessity for certain limitations is apparent; the necessity for additional limitations may be discovered in the actual use of the theory.

General experience with problems of elastic instability indicates that the theory will need to be modified when the buckling stress of the web exceeds the proportional limit of the material, or approximately 12 kips per square inch

for 24S-T alloy. In the tests analyzed in this paper, the buckling stress was always below the proportional limit.

Experimental evidence tends to indicate that the theory of diagonal tension begins to break down when the spacing of the uprights becomes larger than the depth of the beam. The folds then have a pronounced tendency to run from corner to corner of the panel instead of taking the direction indicated by the theory. At the same time the effect of flexibility of the flanges increases rapidly, and there is at present only fragmentary experimental evidence to support the validity of the theory under such circumstances.

The calculations for structural efficiency given in the appendix indicate that, for web systems with double uprights, the structural efficiency tends to zero as the ratio of web thickness to web depth decreases. This conclusion appears reasonable. For web systems with single uprights, however, the calculations indicate that a finite value of structural efficiency is approached as the ratio of web thickness to web depth decreases indefinitely. The calculations also indicate that, as the upright spacing decreases, the structural efficiency approaches that of a web not subjected to buckling. These results for  $h/t \rightarrow \infty$  and for  $d/h \rightarrow 0$  do not appear physically reasonable and are probably caused by failure to recognize the existence of a bending type of failure in single uprights analogous to the bending failure of double uprights. Caution should be used, therefore, in the analysis of web systems with single uprights when the uprights are closely spaced or when the thickness-depth ratio is very small.

#### Correlative Study of Manufacturers' Tests and NACA Tests

In the light of the theory of incomplete diagonal tension in reference 1 as modified by the present paper, a comprehensive study was made of more than 100 tests made by five aircraft manufacturers in order to correlate these tests with the NACA tests described in section I and with the theory. The tests were confined, in general, to determination of the yield load and of the ultimate load; no strain-gage data were included among the available data. The tests furnished sufficient information on several

items to permit a very substantial reduction of the NACA test program and were therefore of considerable usefulness.

Unfortunately, the value of many tests was lessened by the lack of pertinent information. For instance, the shapes of bulb angle stiffeners were not given; it was therefore impossible to calculate accurately the slenderness ratios of the uprights. Again, nominal thicknesses were given instead of actual thicknesses. The results obtained may be in error by as much as 5 percent owing to this source of error alone, because the commercial tolerances are of this order of magnitude. In view of the incompleteness of the data, the individual results obtained from the analyses of these tests should not be too closely scrutinized. For this reason, and also because the analyses are quite voluminous, no details are given in the following discussions. Only final conclusions are given, based on the aggregate of all available data.

Strength of web.— Tests made of square shear panels 0.040 and 0.025 inch thick under pure shear (reference 6) were generally in close agreement with formula (13) for the allowable equivalent shear stress when the sheet was riveted to the outside of the flange angles. When the sheet was clamped between the flange angles, about 10 percent higher stresses were developed.

Among the available manufacturers' test data were eight tests of beams that failed in the web; in all cases, the web was riveted to the outside of the flange angles. The ratio of developed strength to calculated strength was  $0.99 \pm 0.07$ . Corrections for actual properties of material were made, but the corrections were based on uncertain data in some cases.

In the NACA beam tests reported herein, two web failures were observed, discounting the failure in the web of beam 40-3 damaged by accidental contact with an electric welding torch. These webs were clamped between the flange angles and developed  $1.04 \pm 0.03$  times the predicted strength based on formula (12). The developed strength is therefore 5 percent higher than the developed strength of the group of beams with the webs riveted to the outside of the flange angles; whereas, the tests with the square shear panels of reference 6 indicated a gain of 10 percent due to clamping the web between the angles. A possible reason

for the discrepancy is as follows: The flange angles used for the beam tests (section I) were 24S-T aluminum-alloy angles with a fairly smooth finish. The flange angles used for the shear panel tests, on the other hand, were structural-steel angles with the usual rough finish. The angles with the rough finish can probably develop larger friction forces on the sheet than the angles with the smooth finish, and these friction forces relieve the endangered section of the sheet.

The tests discussed thus far include only beams in which the influence of flexibility of the flanges was small ( $C_s < 0.04$ ). The strain-gage tests of beams 25-3 and 25-5 tend to indicate that the factor  $C_s$  gives reasonably correct stress values when  $C_s \approx 0.3$ . A web failure in a beam with  $C_s \approx 0.5$  indicated that large theoretical values of  $C_s$  may tend to be slightly conservative.

The usual method of reducing test results for material properties in excess of minimum guaranteed values was followed in these analyses. This method is based on the properties obtained with standard tensile specimens. The discussion of the results in reference 6 pointed out that this method is questionable and may be in error by as much as 10 percent because the stress-concentration factor for holes is not equal to unity, as commonly assumed for static strength calculations. The test results of reference 6 also indicate that the stress-concentration factor is not constant and sometimes varies in such a manner as to nullify a higher strength shown by a standard tensile specimen.

Strength of uprights.— In single uprights of open section, failure is apparently precipitated when the folds of the web force a localized twisting of the uprights. The twist causes a localized weakening of the uprights; the final failure may therefore be a bending failure. Double uprights are susceptible to the same type of failure and must be separately checked against failure by forced twisting and against column failure. Double as well as single uprights must, of course, be checked against the possibility of failure by local instability.

The empirical formulas (14) and (14a) for upright stresses causing failure by forced twisting were obtained from an analysis of the manufacturers' tests. The tests included all types of stiffener commonly used; namely, bulb angles, plain formed angles, and formed angles with

lips. The stresses in the uprights were calculated by the formulas given in the preceding section. Single uprights were assumed to furnish the equivalent of simple support to the sheet.

It was found by trial that the upright stresses depended primarily on the ratio  $t_U/t$ . Figure 22 presents the plots of test points; the straight lines are graphical representations of formulas (14) and (14a). The figure indicates that the average agreement between the tests and formula (14) varies somewhat with the beam depth. The formula is conservative for the group of beams 10 inches deep becomes gradually less conservative, and becomes finally unconservative for the group of beams 40 inches deep. The formula agrees fairly well with the average of the largest group, that is, the 30-inch group. Within the range covered by the tests, the properties of the material are independent of the absolute sizes. The apparent decrease of ultimate upright stresses with increasing beam depth probably indicates that the ultimate stress depends on a more complicated function than the ratio  $t_U/t$ . The observed decrease of ultimate stress may also be merely accidental and may disappear when the number of tests analyzed becomes much larger than the number now available.

The last explanation is supported by the test results shown in figure 23, which include results for six beams 48 inches deep; the results are in fair agreement with formula (14). The results shown in figure 23 were obtained with beams having double uprights alternating with single uprights, usually of different size. It was assumed, because the uprights were closely spaced, that the stress condition depended on the average effective cross-sectional area of the uprights; the allowable stress was determined separately for double uprights and single uprights. Failure occurred in some beams in the double uprights, and in other beams in the single uprights; the calculations indicated correctly which type of upright should fail first. This fact, as well as the agreement with formula (14) indicated by figure 23, may be taken as vindicating the method of analysis used. Since the 48-inch beams of figure 23 give results in agreement with formula (14), it seems reasonably safe to assume that the formula is valid for all beam depths up to at least 50 inches.

For actual stress analysis, it is recommended that the more conservative formula (14a) be used. As figure 22

indicates, this formula represents fairly well the lower limit of the test data. The two low points in the 20-inch group are probably "wild." The low points in the 30-inch group at low values of  $t_f/t$  suggest that the edge support given by thin uprights should be considered as less than the equivalent of a simply supported edge. (See the appendix.)

Double uprights, as mentioned before, may fail by column action or by forced twisting. Formula (15) for effective column length was based on the NACA tests (section I) and replaces Wagner's theoretical curve of the ratio of theoretical buckling load  $V_T$  to Euler load  $P_E$ . (See references 1 and 2.) Formula (15) indicates that the bracing effect exerted by the web on the uprights is much less than predicted by Wagner's theoretical curve, even when Wagner's curve for pin-ended uprights is applied to uprights attached with two rivets or bolts. In the limiting case of very small spacing of the uprights, Wagner gives a value of  $V_T/P_E = 7$ , while formula (14) gives  $L_e/h_T = 0.5$  corresponding to  $V_T/P_E = 4$ . A partial explanation for the high values obtained by Wagner may lie in the fact that the observed pattern of failure did not agree very well with the simple pattern assumed by Wagner for his strain-energy calculations of the strength of uprights.

As table II indicates, formula (15) tends to give slightly conservative results. Attention is called to the fact, however, that it is important to use actual instead of nominal values of the depth of the outstanding leg in order to obtain correct values for the radius of gyration. Some allowance should be made for the fact that in extruded angles the full thickness of the leg is not carried to the extreme tip.

Particularly instructive are the tests with double uprights included in figure 22. Calculations show that the stresses developed by the double uprights on the 30-inch beams are only fractions (0.3 to 0.6) of the stresses that would produce column failures.

Strength of rivets web-to-flange.— The actual strength of the web-to-flange rivets is usually well in excess of their nominal strength. Part of this excess strength can be traced to the fact that the holes are always drilled oversize to facilitate insertion of the rivet; the actual



cross section of the rivet is therefore larger than the nominal cross section, and the excess is quite large in the smaller sizes of rivets. There is also a change in the strength properties of the rivet as a result of the driving operation (reference 7).

Since the factors giving excess strength to the rivets vary from case to case, it is advisable to base the stress analysis on the nominal strength. Test results should be reduced to the nominal strength analogous to the manner of reducing other test results to minimum guaranteed properties.

The available data included five failures in the web-to-flange rivets. A comparison of the rivet loads computed by formula (16) with the strengths of the rivets based on the drill size indicated that formula (16) was always conservative, the minimum margin found being 2 percent. The use of  $h_e$  instead of  $h_R$  was found to be unconservative in some cases; this fact is mentioned because  $h_e$  is frequently used in all formulas for the design of girders.

Formula (16) is simply a straight-line formula for interpolating between the limiting cases of shear and pure diagonal tension. Under a rigorous interpretation of the theory of incomplete diagonal tension, separate rivet loads would be computed for the diagonal-tension load  $kS$  and the shear load  $(1 - k)S$  and would be added vectorially. The rivet loads obtained in this manner are lower than those obtained by formula (16) except for  $k = 0$  and  $k = 1$ , the maximum difference being about 9 percent at  $k \approx 0.4$ . The rivet loads found by vectorial addition were found to be too low by 5 percent in two cases, compared with the actually developed strengths of the rivets. The use of formula (16) is therefore recommended, although the method of vectorial addition of partial loads may appear to be more rational.

In the tests referred to, the webs were riveted to the outside of the flange angles; it is probable that slightly higher rivet strengths can be developed when the web is clamped between the flange angles.

Strength of rivets upright-to-flange.— The available experimental evidence on the strength of the rivets in the ends of the uprights was fragmentary. It has been

customary to design these rivets either on the basis of the pure diagonal-tension theory or on the basis of the theory that all shear in excess of the critical shear is carried by diagonal tension. These theories give very conservative results and, consequently, there were practically no records of failure of the rivets among the available test data. Indirect evidence was obtained by comparing the strength of successful rivet joints with the calculated loads on them. In the NACA tests of section I, bolts were used instead of rivets because it was considered more important to obtain data on failure of the uprights than data on the failure of rivets.

The load on the end rivets of double uprights is given by formula (17a). There was a record of one failure but, in this case, the nominal strength of the rivets was only about one-half the load calculated by formula (17a). Examination of successful rivet joints indicated that formula (17a) is probably always conservative, but it is impossible to give definite quantitative data because there was too much uncertainty about some of the basic data, particularly on the actual strength of the rivets.

The force on a single upright is theoretically

$$P_U = \sigma_U A_{U_g}$$

Since the upright is eccentrically loaded, some allowance must be made for bending in the rivet. The simplest method of making this allowance is to multiply  $P_U$  by a factor larger than unity to obtain a design load. Among the available test data, were data on two failures of end rivets in single uprights. These tests indicated that the value of  $P_U$  given should be doubled to obtain a design load. The calculations were uncertain, chiefly because the shape of the cross section of the bulb-angle uprights was not known and consequently  $A_{U_g}$  could not be calculated with any degree of certainty. A definitely conservative design procedure for these two cases would be to apply formula (17a). It is recommended, therefore, that formula (17a) be used for single uprights as well as for double uprights until additional experimental evidence is obtained.

Rivets upright-to-web.— The design of the rivets between uprights and web rests on a very uncertain basis

for single uprights as well as for double uprights. Design criteria are either of an indefinite nature or, although definite theoretically, cannot be readily translated into specific design requirements.

For single uprights, a possible criterion for designing the rivets is given by the consideration that the rivet line should give to the sheet as much support as possible in order to increase the buckling stress. The equivalent of a simply supported edge can possibly be obtained with a practical rivet pitch, but the number of rivets necessary to achieve this purpose is not known at present and probably varies considerably, depending on the interpretation of the term "equivalent of a simply supported edge." One method of design (reference 8) is to choose the rivet spacing such that the web does not buckle between rivets under the compressive stress acting on the uprights. The question arises, however, whether it is necessary to prevent the occurrence of this buckling until the maximum load has been reached or whether it might be permissible to let buckling begin after the design yield load. An upper limit for the rivet pitch is given by the criterion  $p < d/4$  suggested in reference 1. This criterion is based on the assumptions that one fold begins at each upright and that the rivet pitch must be less than one-fourth of the wave length in order to break up the wave pattern. The assumption that one fold starts at each upright does not hold for all possible design proportions, although for aluminum alloys it probably holds over most of the practical range.

In double uprights expected to fail as columns, the rivets should theoretically be designed to withstand the longitudinal shear force in the upright. This shear force cannot be calculated unless the deformation of the uprights at the instant of failure is known, and the calculation of this deformation is beyond the limitations of the linearized theory of column action. For columns made of steel with a well-defined yield point, some progress has been made in calculating the deformations. For materials with curved stress-strain diagrams such as aluminum alloys, the calculations will be much more difficult; they are further complicated by the bracing action of the web and by the fact that the strength of the rivets affects the strength of the uprights, as shown by the tests on beams 40-4a, 40-4b, and 40-4c. On the meager evidence given by the three NACA tests, it is suggested that the total strength of the rivets in double shear be made at least

equal to the load  $P_T$  on the upright and preferably equal to twice this load.

In double uprights expected to fail by forced twisting, more attention should perhaps be given to close spacing of the rivets than to the strength of the rivets.

Permanent set.— In the manufacturers' tests analyzed, permanent set was determined by one or several of the following criterions: loss of tautness of the web, determined by feel; permanent buckling of the web as a whole, determined by a straight edge; appearance of definitely visible shear wrinkles in the corners; and, finally, visible permanent set in the uprights. One report mentions that the methods employed gave lower yield loads than the deflection readings, but there is no record of deflection readings beyond this passing mention. The data on yield loads given in the test reports analyzed have, therefore, the common feature that they are not based on quantitative measurements. Subjective methods of the type used may conceivably yield reasonably consistent results when employed by one engineer within the compass of one test series. Results obtained by different engineers, on the other hand, may be expected to show a large amount of scatter.

Examination of separate test series indicated large scatter within each test series; the experimental shear stresses producing permanent set are therefore shown as a composite plot in figure 24. The shear stresses were calculated by the formula

$$\tau = S(1 + kC_1)(1 + kC_2)/h_s t \quad (19)$$

The correction factor  $kC_1$  was always fairly small, but the factor  $kC_2$  was greater than 0.5 for a number of beams and was 0.76 for one beam. The test points in figure 24 indicate that permanent set begins at shear stresses as low as 11 or 12 kips per square inch. This result is in agreement with the results obtained from the measurements of permanent deflections in the NACA tests (table II).

Test engineers appear to be more or less in agreement that a severe weight penalty would be imposed upon the designer if he were required to design a beam in such a manner that no wrinkles remain perceptible after the design

yield load has been applied once. A requirement of this nature would also appear to be not entirely consistent with the fact that simple members may be designed to reach, at the design yield load, the specification yield stress of the material. The specification yield point is not defined as the minimum perceptible permanent set but as a well-defined, fairly large permanent set. In view of these considerations, it would seem advisable to substitute for the somewhat vague concept of permanent set two separate concepts, namely, permanent shear deflection and permanent wrinkles.

It seems reasonable to assume that the permanent shear deflection can be calculated by relating the shear stress given by formula (19) directly to the effective shear stress-strain curve of the material. The only reservation to be made is that the factor  $C_s$  must not be too large, because a large factor  $C_s$  is associated with a large concentration of shear stress, and the shear deflection of the beam is a function of the average shear stress rather than the maximum shear stress.

In reference 9, dealing with torsion tubes of 17S-T alloy, it was suggested that the yield shear stress be defined as the stress at which  $\bar{\epsilon}/\epsilon = 2/3$ . If this suggestion is followed, the curve of figure 21 gives a yield stress of 24 kips per square inch. This value is in reasonable agreement with the yield stresses of 22.5 kips per square inch for 17S-T alloy mentioned in reference 3 and 23.3 kips per square inch given in reference 9. The elastic limit of 24S-T alloy lies at 12.5 kips per square inch if figure 21 is used as basis.

The results shown in figure 24 indicate that the shear stresses producing permanent wrinkles lie anywhere between the elastic limit and the yield stress for sheets less than 0.06 inch thick. For thicker sheets, the stress producing permanent wrinkles is nearer the yield stress, but the number of tests in this region is small. It is interesting to note that the lower limit of the scatter band in figure 24 may also be explained by referring to the experimental results of Wagner and Lahde given in reference 10. These experiments showed that the maximum stresses around the edges of a sheet panel in shear are about twice as high as the average stresses.

Permanent wrinkles may be caused by compressive stresses in the sheet where the joggle of the upright leaves the sheet

without support. This type of wrinkle can probably be predicted by the method used for predicting the buckling of sheet between rivets (reference 8).

Langley Memorial Aeronautical Laboratory,  
National Advisory Committee for Aeronautics,  
Langley Field, Va.

## APPENDIX

### STRUCTURAL EFFICIENCIES OF DIAGONAL-TENSION WEBS

The formulas for stress analysis presented in this paper are reasonably adequate for the design of the web and of the uprights. It seems appropriate, therefore, to re-examine the question of structural efficiencies obtainable by balanced designs in which the web and the uprights fail simultaneously.

Within the range of validity of the formulas given, the stresses developed depend only on the proportions of the web systems and not on their absolute sizes. The range of validity of the formulas may be assumed at least to equal the range of the tests, that is, to cover web depths up to 50 inches and web thicknesses up to 0.091 inch, subject to the limitation that  $\tau_{cr}$  must be less than the proportional limit of the material. All curves shown in the appendix comply with this limitation.

In order to reduce the large amount of computational work, a standard shape of cross section was assumed for the uprights. For simplicity, a simple angle was chosen. The outstanding leg was assumed to be twice as wide as the leg attached to the web to give a section efficient in bending. The width-thickness ratio of the outstanding leg was assumed to be  $b/t_U = 12$ , to eliminate the possibility of elastic instability of the free edge. With these assumptions, the following relations were obtained for double uprights:

$$A_U = 3bt_U = b^2/4$$

$$\rho = 0.471b$$

and for single uprights:

$$A_U = b^2/8$$

$$A_{Ue} = b^2/16$$

The material was assumed to be 24S-T alloy. The strength values and the column curve were taken from reference 5. The rivet factor was taken as  $C_R = 0.80$ . Formula (14a) was used to obtain the allowable stress for twisting failure.

The buckling stresses were computed by the formula

$$\tau_{cr} = K_1 \tau_{cr}(\text{supp})$$

where  $\tau_{cr}(\text{supp})$  is the buckling stress for panels with simply supported edges given by figure 15 and  $K_1$  is a factor depending on the uprights as shown by figure 25. The curve for  $K_1$  is based on very limited experimental evidence but, since changes in  $K_1$  do not affect the final result very much, the curve may be used for most practical purposes. The particular manner in which the factor  $K_1$  was employed here implies the assumption that the method of edge support along the flanges is the same as along the uprights.

On the basis of the assumptions outlined, a number of web systems were designed such that the webs and the uprights would fail simultaneously. Curves of the structural efficiencies of the web systems with double uprights are shown in figure 26. The measure of efficiency used is the strengths of the webs divided by the volume of material per inch run  $V$ , or the average shear stress based on all the material in the web system. The calculations showed that at large values of  $h/t$  (4000 and 2000) double uprights fail by column bending. The curves pertaining to failure by bending are concave downward in figure 26. As  $h/t$  decreases, a point is reached where the uprights fail by twisting before they can fail by bending. The curves pertaining to twisting failure are concave upward in figure 26. For  $h/t = 1000$ , the curve for bending failure and the curve for twisting failure intersect twice. When

$d/h$  is either near unity or when it is small, bending failure is decisive. For intermediate values of  $d/h$ , twisting failure is decisive; the decisive type of failure in each case is indicated by full lines in figure 26. At  $h/t = 500$ , twisting failure is decisive except at small values of  $d/h$ .

Inspection of figure 26 leads to several conclusions of general interest. One conclusion is that the structural efficiency increases as the value of  $h/t$  decreases. The reason is twofold: As  $h/t$  decreases, the state of stress in the web approaches more closely the state of shear, and the allowable equivalent shear stress increases. At the same time, the load imposed on the uprights decreases, and smaller uprights may be used.

Another conclusion that may be drawn from figure 26 concerns the upright spacing giving the greatest structural efficiency. At very large values of  $h/t$ , the greatest efficiency is obtained when  $d/h$  equals unity. Some caution should be used in the practical application of this conclusion, because the calculations on which figure 26 is based neglect the influence of flexibility of the flanges.

At smaller values of  $h/t$ , when twisting becomes the decisive type of failure, the best efficiency is obtained by using closely spaced uprights. The curves for twisting failure continue to rise as  $d/h$  decreases, and the strength-volume ratio approaches the limiting value  $C_{RTult}$ . The onset of column failure, however, makes it impossible to realize the high efficiency that could be obtained if failures were confined to twisting failures.

The results of the calculations for single uprights are shown in figure 27. The curves have a somewhat unusual appearance and are apparently of an oscillatory nature. The curves tend toward the limiting value of  $S/V = C_{RTult}$  in the same manner as the corresponding curves for twisting failure of double uprights in figure 26. The curves for double uprights are, however, prevented from reaching the limiting value  $C_{RTult}$  by the fact that bending failure becomes controlling; the theoretical curves for single uprights, on the other hand, can actually reach the limiting value because the method of analysis used does not recognize the possibility of bending failures in single uprights. No doubt such failures are possible; in the limiting case of very closely spaced uprights, the theory of buckling of an



orthotropic plate (reference 1) should be applicable. Because little is known about the validity of this theory, no attempt was made to take into account the possibility of bending failures in single uprights. In view of this fact, results concerning closely spaced single uprights should be considered with great caution.

Failure to take into account the possibility of bending failures in single uprights is probably also responsible for the fact that figure 27 indicates a finite value of structural efficiency for  $h/t \rightarrow \infty$ , while the structural efficiency of webs with double uprights decreases indefinitely as  $h/t$  increases.

In the design of web systems, the given quantities are normally the shear load  $S$  and the depth  $h$ . It is customary to combine these quantities into the structural index  $\sqrt{S}/h$ , which is based on the principle of structural similarity stating that stresses in geometrically similar structures are identical when the loads are proportional to the square of the linear scale ratio. Structures having the same index values have the same stresses.

In figure 28, the strength-volume ratios for webs with double uprights and for webs with single uprights are plotted against the structural index. The discontinuity in the curves for single uprights is caused by reaching the limiting stress value of 50 kips per square inch in the uprights. The test range indicated is the range of manufacturers' tests, which includes that of the NACA beam tests. Well within the test range, there is little to choose between single uprights and double uprights. Near the borders of the test range, the single uprights become more efficient than the double uprights. It should be borne in mind, however, that the unrestricted validity of the formula for twisting failure becomes questionable near the borders of the test region. The curves in figure 28 show more clearly than figures 26 and 27 the manner in which the structural efficiency varies with the  $h/t$  ratio. This comparison is possible because, for practical purposes, the ratio  $h/t$  may be used instead of the index value  $\sqrt{S}/h$  when only structures made of the same material are being studied.

Of considerable practical interest is the magnitude of the reinforcement ratio  $A_f/dt$ . Figure 29 shows graphically how the reinforcement ratio varies with the

structural index. These curves may be used to obtain an estimate of the amount of stiffening required in a given design. Since the shape of the upright-chosen will probably differ from the standard shape assumed for these calculations, a final analysis must be made in most cases to check the strength of the web system.

#### REFERENCES

1. Kuhn, Paul: Investigations on the Incompletely Developed Plane Diagonal-Tension Field. Rep. No. 697, NACA, 1940.
2. Wagner, Herbert: Flat Sheet Metal Girders with Very Thin Metal Web. Pt. II. Sheet Metal Girders with Spars Resistant to Bending - Oblique Uprights - Stiffness. T. M. No. 606, NACA, 1931.
3. Moore, R. L.: An Investigation of Web Buckling in Some Aluminum Alloy Plate Girders with Additional Information on Vertical Deflections, Stress Distribution and Ultimate Strengths. P.T. Rep. No. 39-47, Aluminum Res. Lab., Aluminum Co. of America, Sept. 15, 1939.
4. Timoshenko, S.: Strength of Materials. Pt. II. D. Van Nostrand Co., Inc., 1930, p. 607.
5. Anon.: Strength of Aircraft Elements. ANC-5, Army-Navy-Civil Committee on Aircraft Requirements. U. S. Govt. Printing Office, Oct. 1940.
6. Kuhn, Paul: Ultimate Stresses Developed by 24S-T Sheet in Incomplete Diagonal Tension. T.N. No. 833, NACA, 1941.
7. Brueggeman, Wm. C.: Mechanical Properties of Aluminum-Alloy Rivets. T.N. No. 585, NACA, 1936.
8. Miles, Alfred S., and Newell, Joseph S.: Airplane Structures. Vol. I. 2d ed., John Wiley & Sons, Inc., 1938, p. 330.
9. Stang, Ambrose H., Ramberg, Walter, and Back, Goldie: Torsion Tests of Tubes. Rep. No. 601, NACA, 1937.
10. Lahde, R., and Wagner, H.: Tests for the Determination of the Stress Condition in Tension Fields. T.M. No. 809, NACA, 1936.

TABLE I. - PROPERTIES OF NACA BEAMS

Beam	h (in.)	h <sub>o</sub> (in.)	h <sub>R</sub> (in.)	h <sub>U</sub> (in.)	t (in.)	d (in.)	$\frac{d}{h}$	Uprights (nominal size) (in.)	A <sub>U</sub> = A <sub>Uo</sub> (sq in.)	$\frac{A_{Uo}}{dt}$	$\rho$ (in.)	Flanges (2Ls) (in.)	$\omega d$	$\tau_{cr}$ ( $\frac{kips}{sq\ in.}$ )
40-1	41.1	40.0	38.6	38.6	0.0425	10.0	0.25	$\frac{9}{16} \times \frac{1}{8}$	0.338	0.795	0.256	$2 \times 2 \times \frac{1}{4}$	1.12	1.83
40-2	41.1	40.0	38.6	38.6	.0425	10.0	.25	$1 \times \frac{5}{8}$	.384	.903	.490	$2 \times 2 \times \frac{1}{4}$	1.12	1.83
40-3	43.1	41.4	40.6	38.6	.0392	20.0	.49	$1 \times \frac{5}{8}$	.384	.490	.490	$3 \times 3 \times \frac{5}{16}$	1.52	.42
40-4a	43.1	41.4	40.6	38.6	.0390	20.0	.49	$\frac{3}{4} \times \frac{5}{8}$	.353	.454	.351	$3 \times 3 \times \frac{5}{16}$	1.52	.42
40-4b	43.1	41.4	40.6	38.6	.0390	20.0	.49	$\frac{3}{4} \times \frac{5}{8}$	.353	.454	.351	$3 \times 3 \times \frac{5}{16}$	1.52	.42
40-4c	43.1	41.4	40.6	38.6	.0390	20.0	.49	$\frac{3}{4} \times \frac{5}{8}$	.353	.454	.351	$3 \times 3 \times \frac{5}{16}$	1.52	.42
25-1	26.1	25.0	23.9	23.9	.0102	10.0	.40	$\frac{1}{2} \times \frac{1}{2} \times \frac{1}{16}$	.123	1.206	.232	$2 \times 2 \times \frac{3}{16}$	1.24	.11
25-2	26.1	25.0	23.9	23.9	.0105	20.0	.80	$\frac{1}{2} \times \frac{1}{2} \times \frac{1}{16}$	.123	.586	.232	$2 \times 2 \times \frac{3}{16}$	2.51	.04
25-3	26.1	25.0	23.9	23.9	.0116	10.0	.40	$\frac{13}{32} \times \frac{1}{2} \times \frac{1}{16}$	.110	.952	.167	$2 \times 2 \times \frac{3}{16}$	1.29	.14
25-4	26.1	25.0	23.9	23.9	.0153	10.0	.40	$\frac{13}{32} \times \frac{1}{2} \times \frac{1}{16}$	.114	.747	.182	$2 \times 2 \times \frac{3}{16}$	1.38	.25
25-5	26.1	25.0	23.9	23.9	.0150	20.0	.80	$\frac{9}{16} \times \frac{5}{8} \times \frac{1}{8}$	.269	.897	.247	$2 \times 2 \times \frac{3}{16}$	2.72	.08
25-6	26.1	25.0	23.9	23.9	.0162	20.0	.80	$\frac{9}{16} \times \frac{5}{8} \times \frac{3}{32}$	.206	.635	.241	$2 \times 2 \times \frac{3}{16}$	2.79	.09
25-7	26.1	25.0	23.9	23.9	.0402	10.0	.40	$\frac{5}{8} \times \frac{5}{8} \times .040$	.101	.252	.291	$2 \times 2 \times \frac{3}{16}$	1.75	1.12

TABLE II

## SUMMARY OF NACA TEST RESULTS

Beam	P <sub>cr</sub> (kips)	P <sub>ult</sub> (kips)	Failure	$\frac{P_{ult}}{\text{Calc } P_{ult}}$	$\frac{S'}{S}$
40-1	3.11	27.40	Uprights	1.03	0.995
40-2	3.11	39.30	Flange	(a)	.995
40-3	.68	37.00	<sup>b</sup> Web	(a)	.978
40-4a	.67	30.30	Uprights	.99	.976
40-4b	.67	32.10	Uprights	1.05	.976
40-4c	.67	35.70	Uprights	1.17	.976
25-1	.03	6.80	Web	(a)	.934
25-2	.01	6.30	Uprights	1.37	.928
25-3	.04	7.60	Web	(a)	.939
25-4	.10	7.80	Uprights	1.06	.952
25-5	.03	10.90	None	(a)	.952
25-6	.09	10.00	Uprights	1.22	.953
25-7	1.13	12.70	<sup>c</sup> Uprights	.96	.980

<sup>a</sup>Uprights did not fail.<sup>b</sup>Premature failure owing to accidentally damaged web.<sup>c</sup>Failure precipitated by forced twisting. Ultimate failure at end of one upright.

TABLE III

## STRENGTH OF UPRIGHT-TO-WEB RIVETS (NACA TESTS)

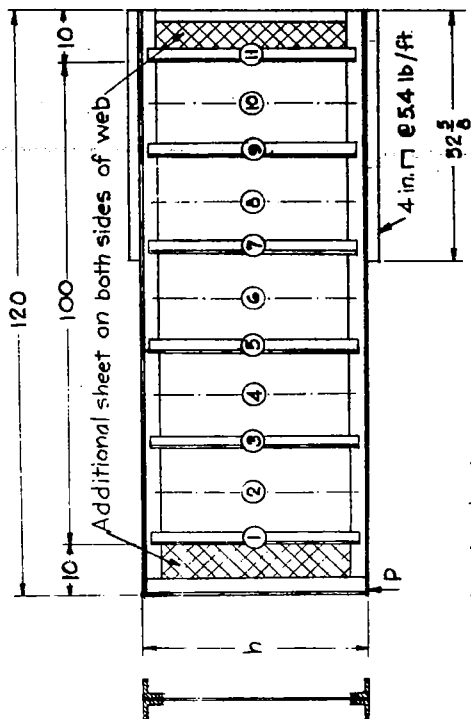
Beam	Rivets (Al7S-T)		Rivet strength $S_R$ (kips)	Calc $\sigma_u$ at ultimate $\left(\frac{\text{kips}}{\text{sq in.}}\right)$	Calc $P_u$ at ultimate (kips)	$\frac{S_R}{\text{Calc } P_u}$	$\frac{P_{ult}}{\text{Calc } P_{ult}}$
	Quantity	Size (in.)					
40-1	12	$\frac{1}{8}$	7.94	7.90	2.67	2.97	1.03
40-2	12	$\frac{1}{8}$	7.94	11.90	4.57	1.74	(b)
40-3	12	$\frac{1}{8}$	7.94	24.20	9.30	.85	(b)
40-4a	12	$\frac{1}{8}$	7.94	19.60	7.00	1.13	.99
40-4b	12	$\frac{5}{32}$	12.45	21.20	7.48	1.66	1.05
40-4c	23	$\frac{5}{32}$	23.85	24.20	8.56	2.79	1.17
25-1	5	$\frac{1}{8}$	3.30	18.30	2.25	1.47	(b)
25-2	5	$\frac{1}{8}$	3.30	30.00	3.69	.90	1.37
25-3	5	$\frac{1}{8}$	3.30	22.20	2.45	1.35	(b)
25-4	5	$\frac{1}{8}$	3.30	18.20	2.08	1.59	1.06
25-5	5	$\frac{1}{8}$	3.30	(c)	(c)	(c)	(b)
25-6	6	$\frac{5}{32}$	6.22	28.00	5.77	1.08	1.22
25-7	8	$\frac{1}{8}$	5.30	9.60	.97	5.47	.96

<sup>a</sup>Double shear.<sup>b</sup>Uprights did not fail.<sup>c</sup>Test stopped before failure.

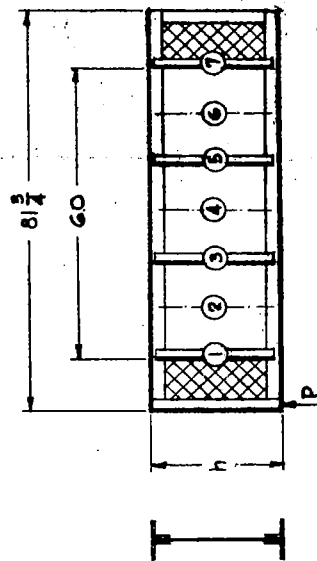
TABLE IV  
PERMANENT BEAM DEFLECTIONS (NACA TESTS)

Beam	P (kips)	$\tau$ $\left(\frac{\text{kips}}{\text{sq in.}}\right)$	Total deflection of tip (in.)	Shear deflection of tip (in.)	Permanent set of tip dial (in.)	P <sub>ult</sub> (kips)
40-1	20.00	11.76	0.395	0.296	<sup>s</sup> 0.004	27.40
40-2	15.00	8.82	.298	.224	.000	39.30
40-3	15.00	9.24	.329	.285	-.002	37.00
40-4a	15.00	9.30	.371	.327	.006	30.30
25-1	4.00	15.68	.477	.401	.019	6.80
25-2	1.50	5.73	.169	.139	.002	6.30
25-3	4.00	13.78	.394	.319	.007	7.60
25-4	7.00	18.26	.570	.440	.009	7.80
25-5	4.00	10.67	.323	.249	.001	<sup>a</sup> 10.90

<sup>a</sup>Test stopped before failure.



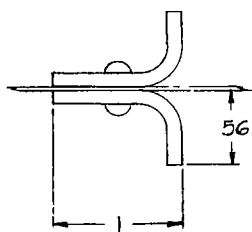
(a) 40-inch beams.



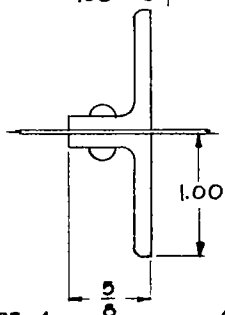
(b) 25-inch beams.

Figure 1.—General dimensions of test beams.

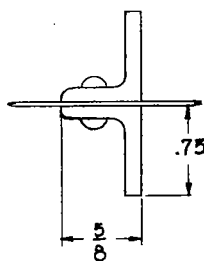
Beam 40-1  
 $A_U = 0.338$  sq in.



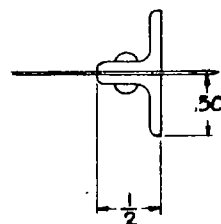
40-2 & 40-3  
 $.384$  sq in.



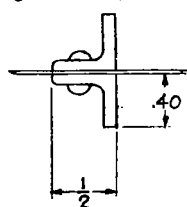
40-4  
 $.353$  sq in.



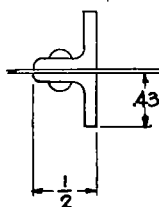
25-1 & 25-2  
 $.123$  sq in.



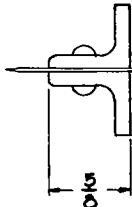
Beam 25-3  
 $A_U = 0.110$  sq in.



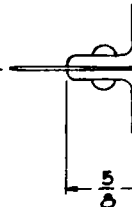
25-4  
 $.114$  sq in.



25-5  
 $.269$  sq in.



25-6  
 $.206$  sq in.



25-7  
 $.101$  sq in.

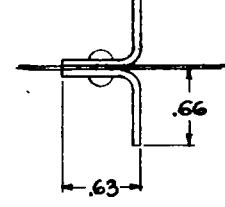


Figure 2.—Cross sections of uprights.

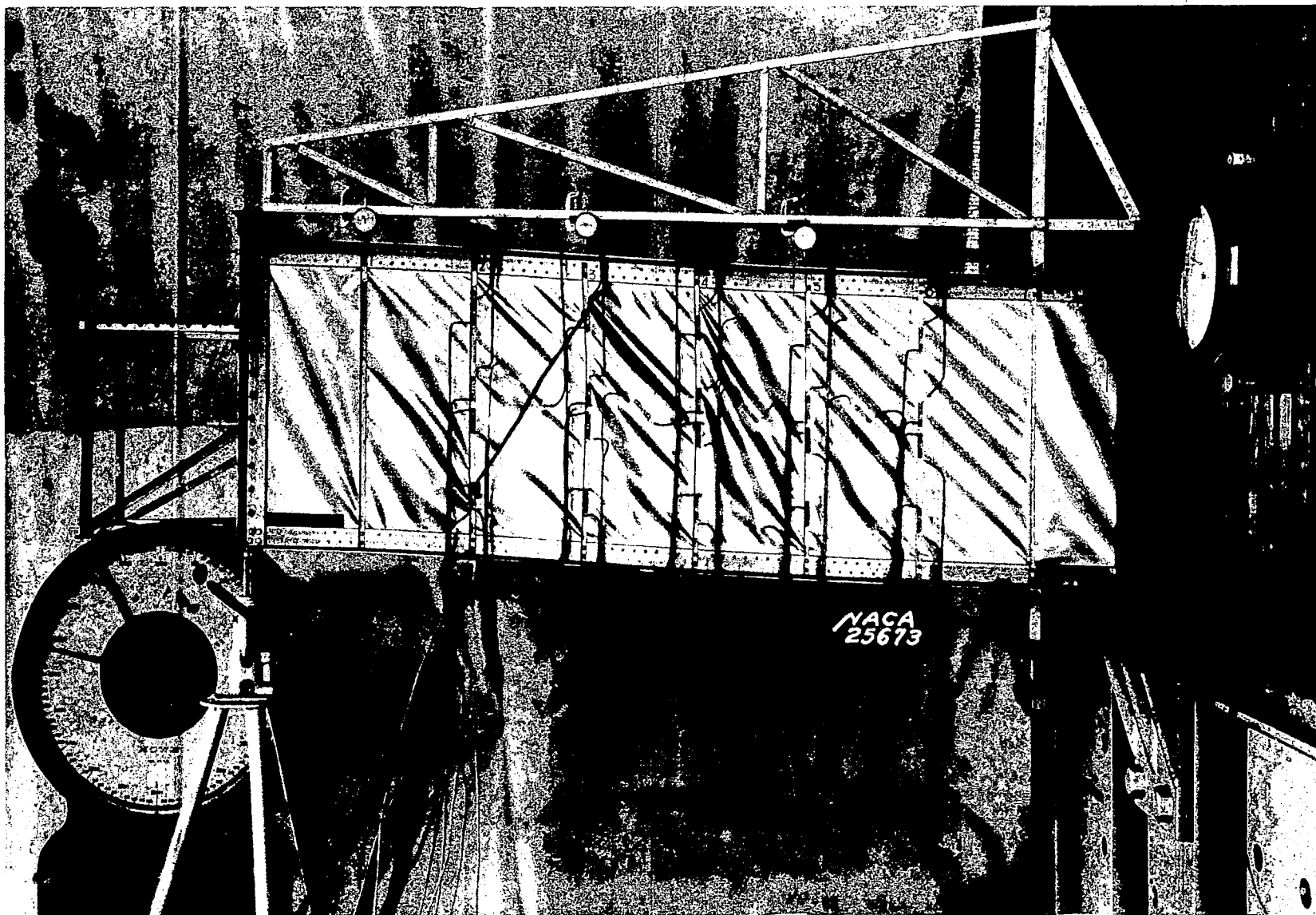


Fig. 3

Figure 3.- Beam 25-1 after failure. Notice web rupture in third bay from tip.

● - Points of attachment of truss.

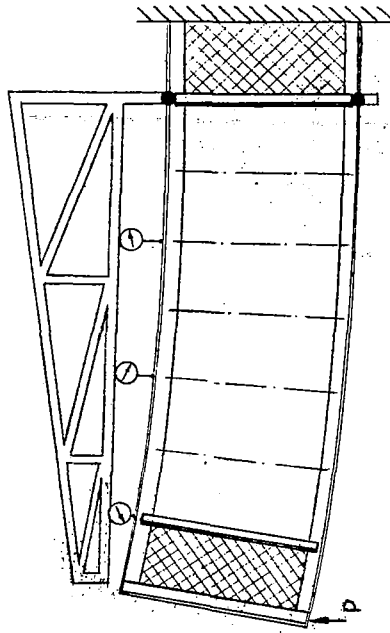


Figure 4.-Set-up for measuring beam deflections.

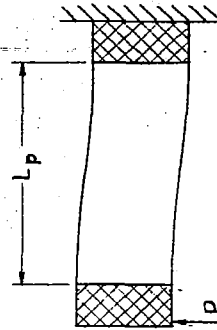


Figure 9.- Portal-frame action.

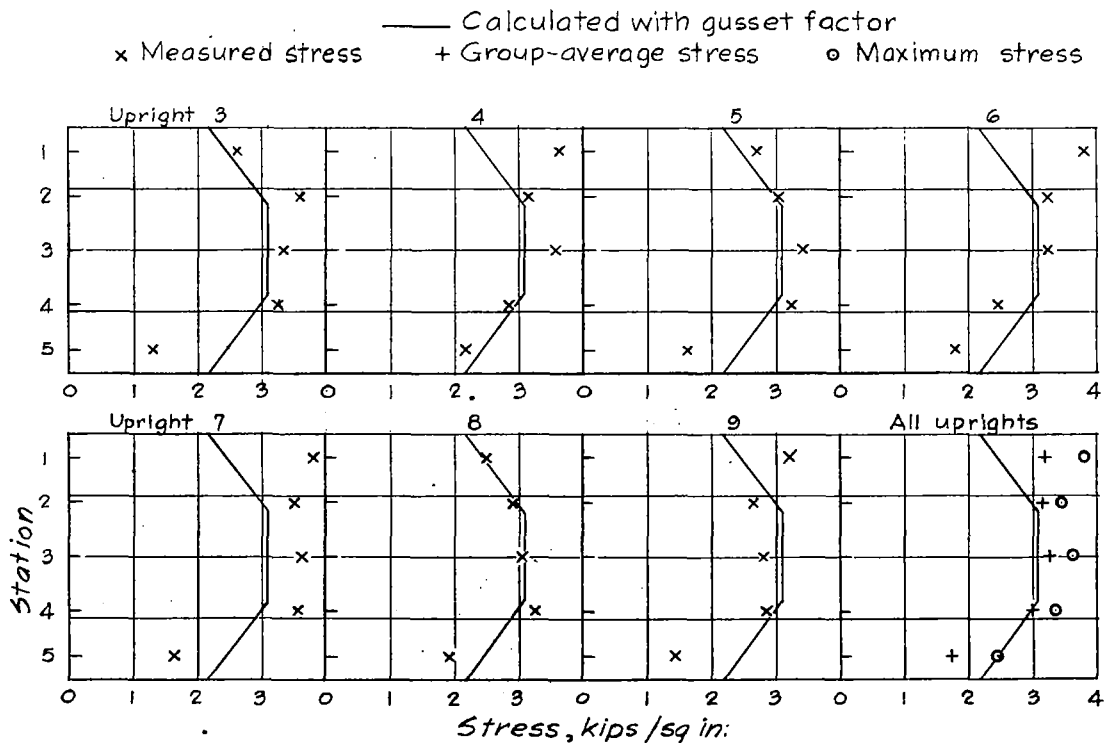


Figure 10.- Transverse distribution of stresses in uprights of beam 40-1 at P=15 kips.



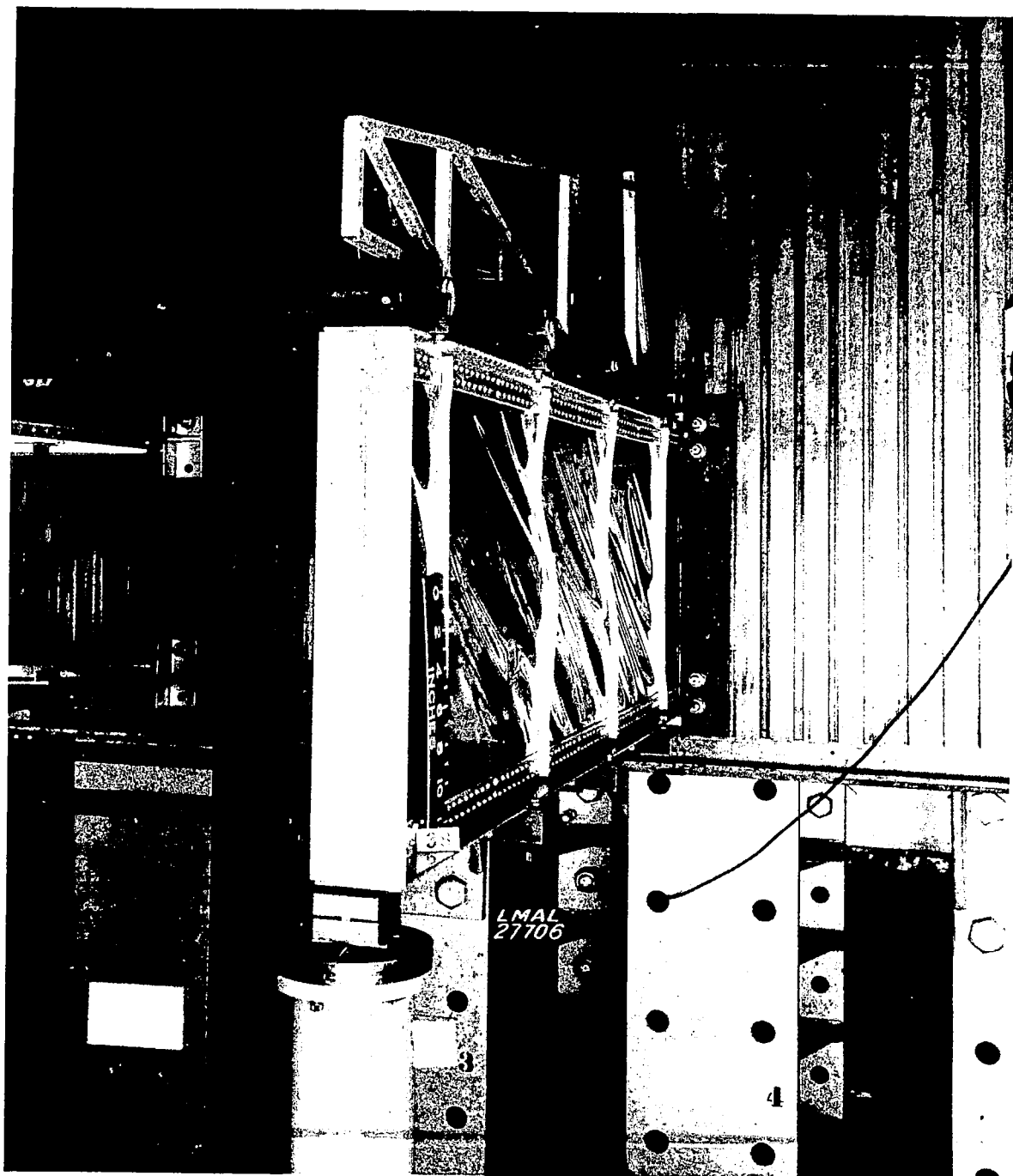


Figure 5.- Beam 25-6 after failure of uprights by column bending.

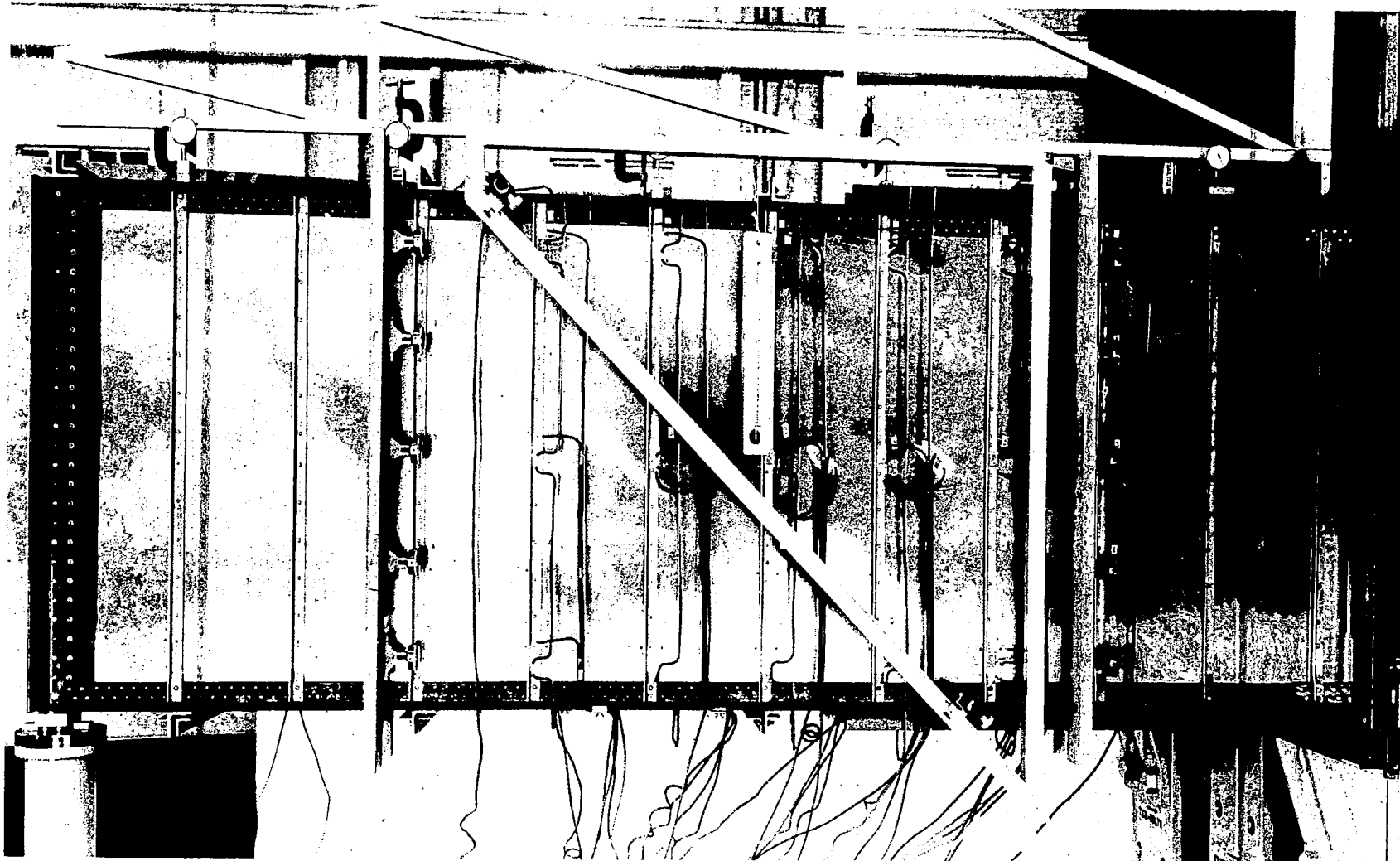


Figure 6.- Special set-ups on beam 40-1.



Figure 7.- Beam 25-7 after failure of uprights by forced twisting.

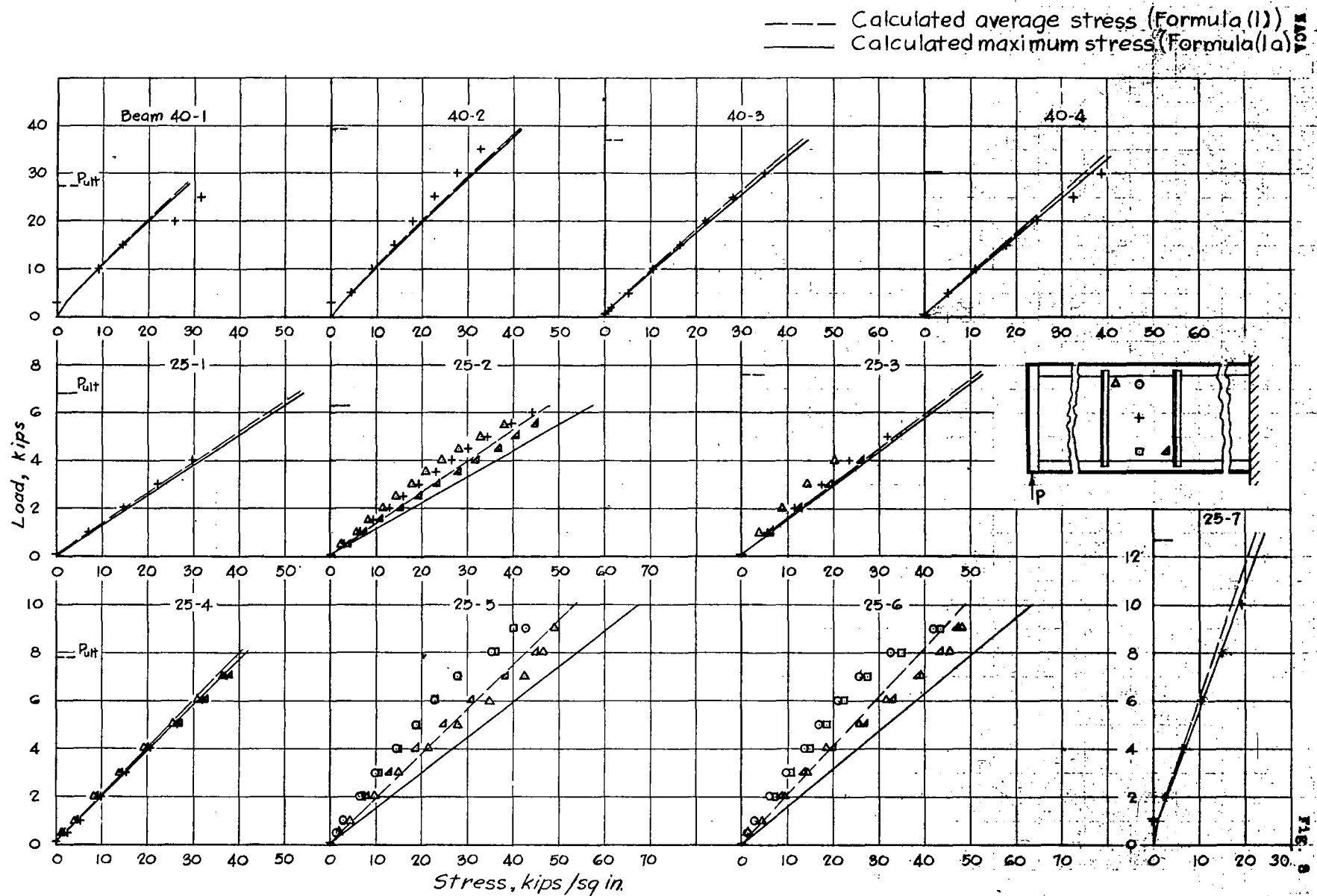


Figure 8.— Stresses in webs—group averages.

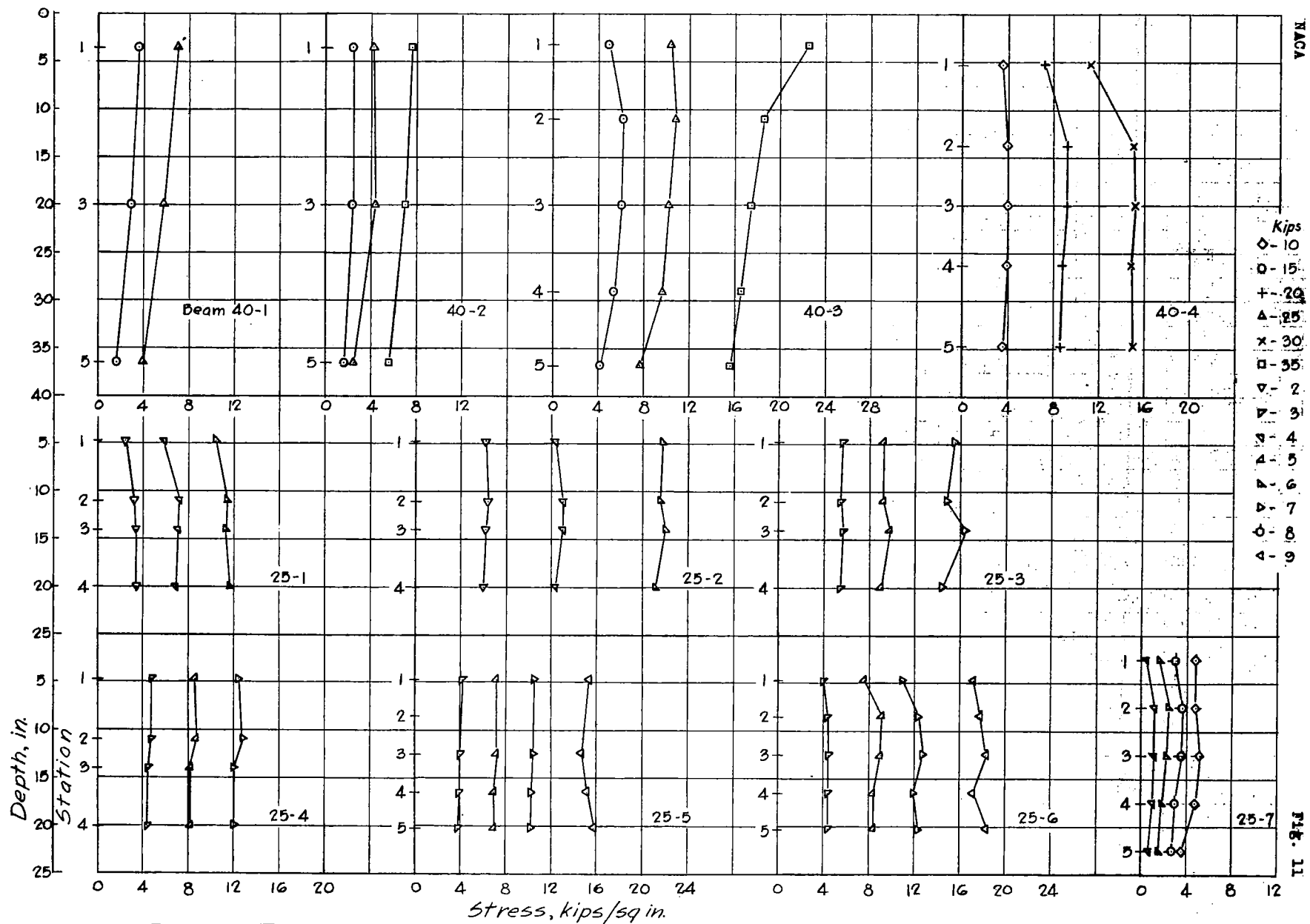


Figure 11 - Transverse distribution of group-average stresses in uprights.

+ Group-average stress  
o Maximum stress

— Calculated

----- Allowable stress for bending

----- Allowable stress for twisting (Formula (14a))

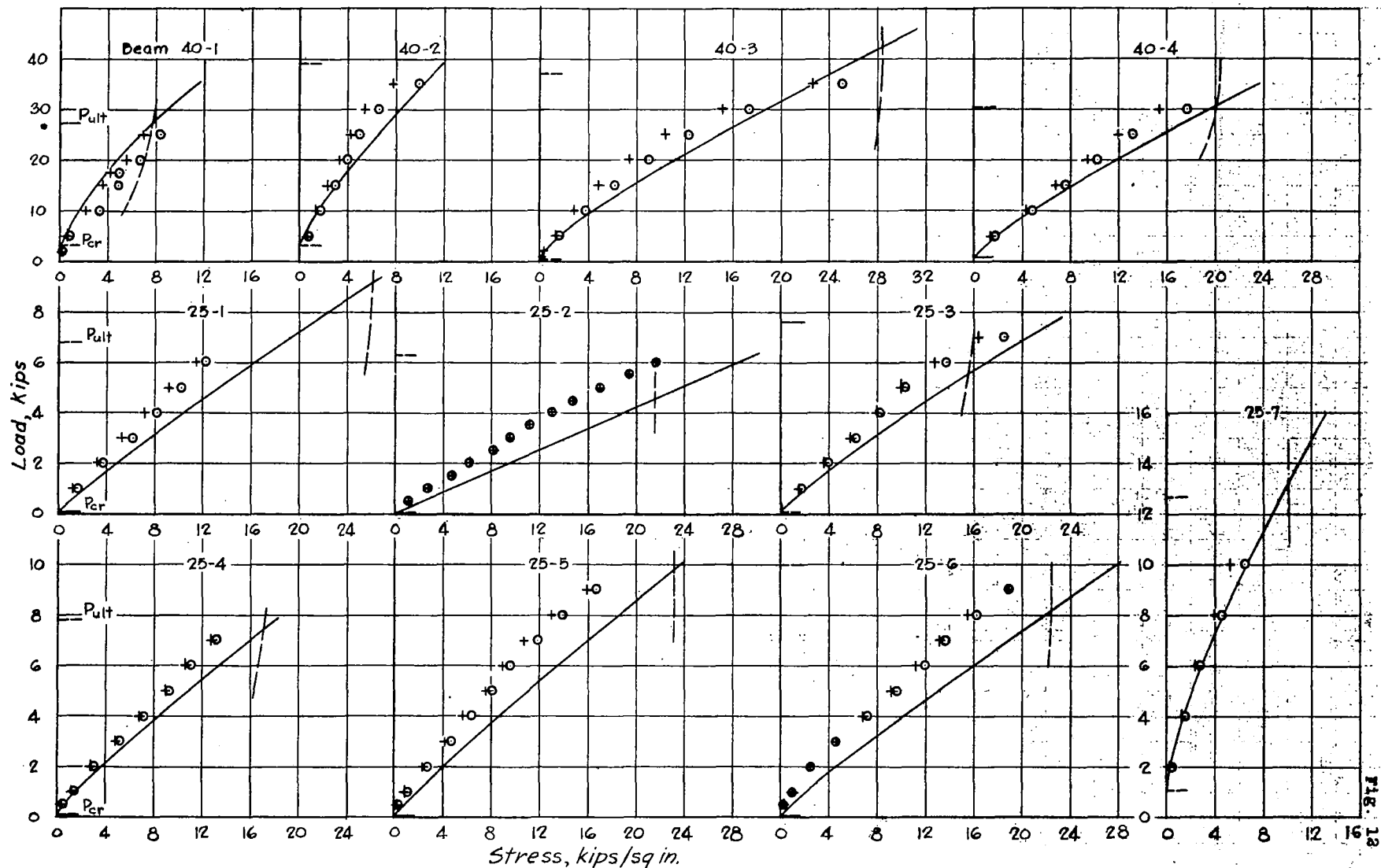


Figure 12.— Stresses in uprights.

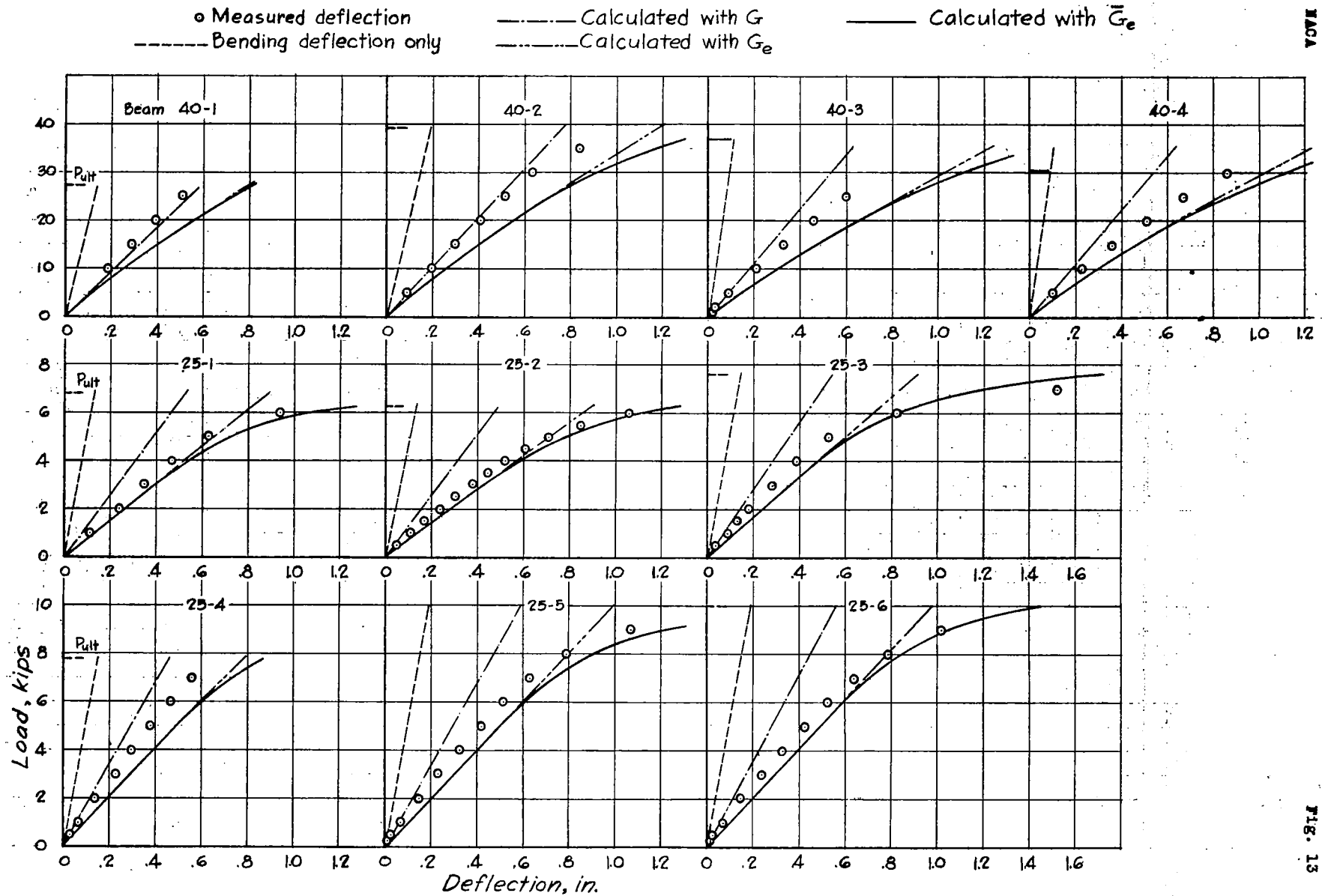


Figure 13.— Load-deflection curves.

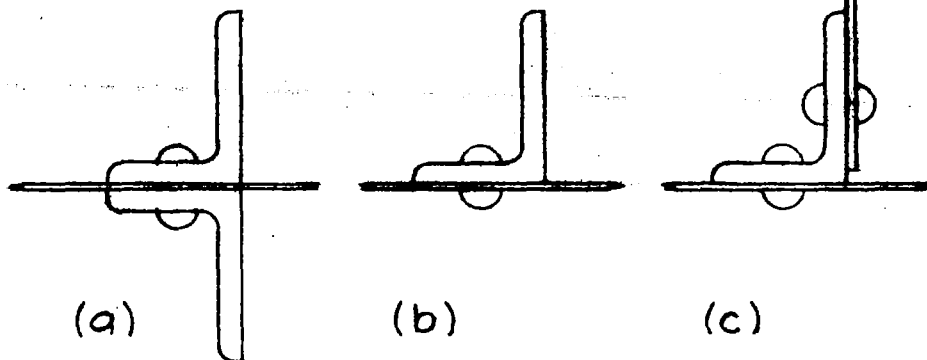


Figure 14.— Basic types of upright.

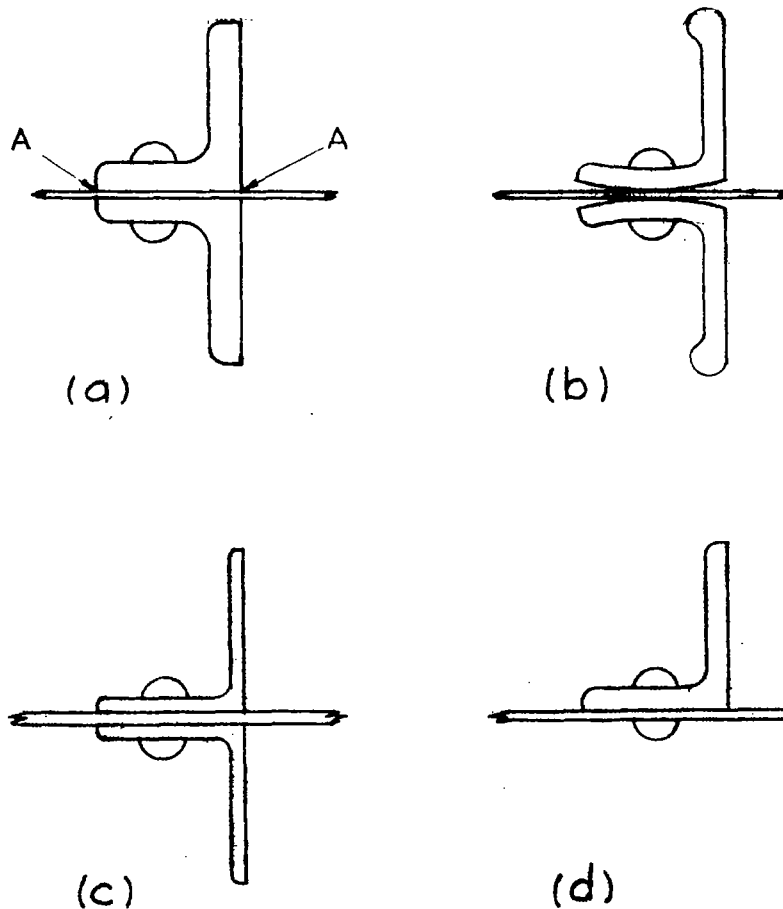


Figure 16.—Uprights producing different edge conditions of web.



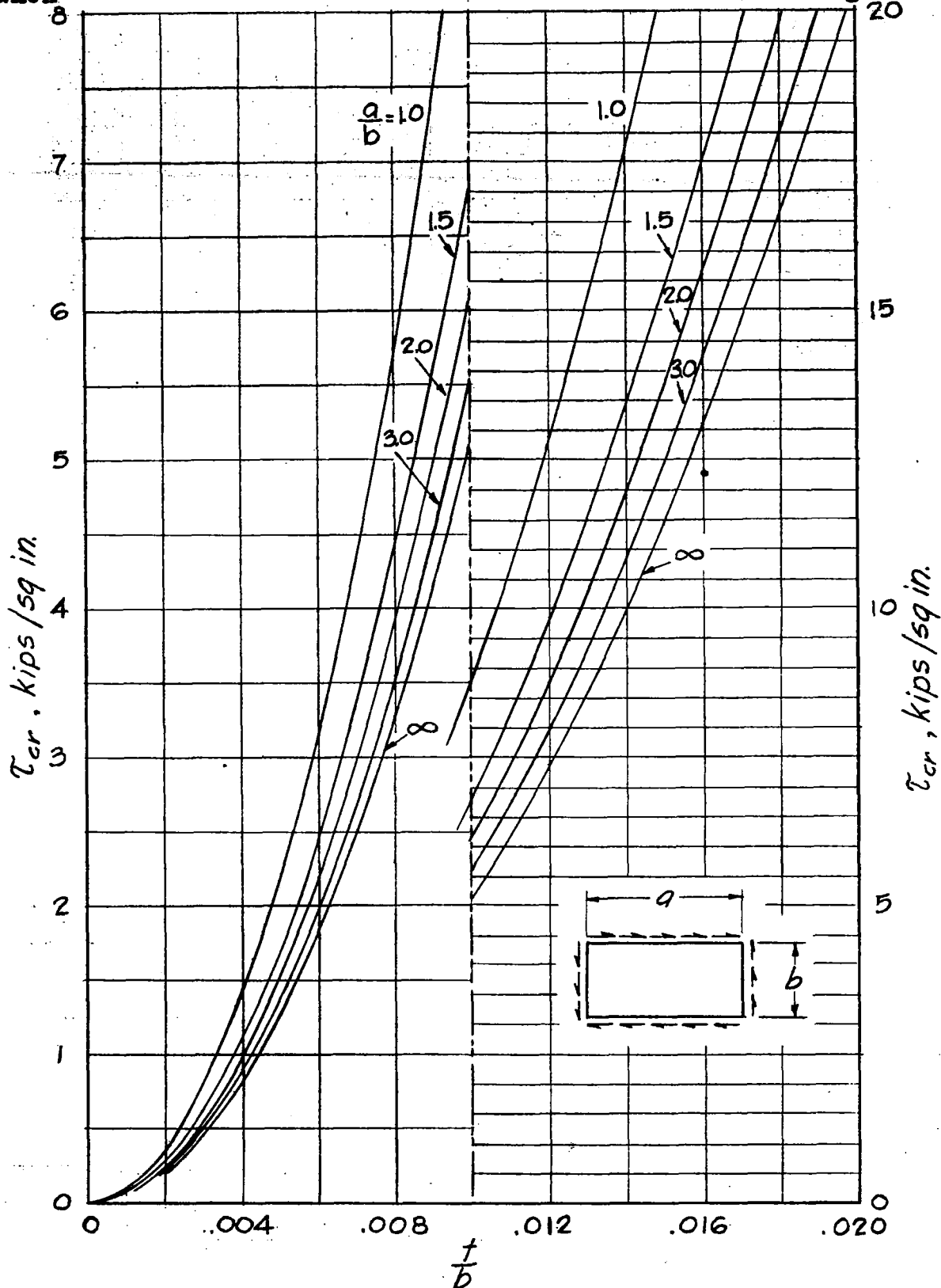


Figure 15. — Critical shear stress for aluminum-alloy sheet with simply supported edges ( $E=10,600$  kips/sq in.).

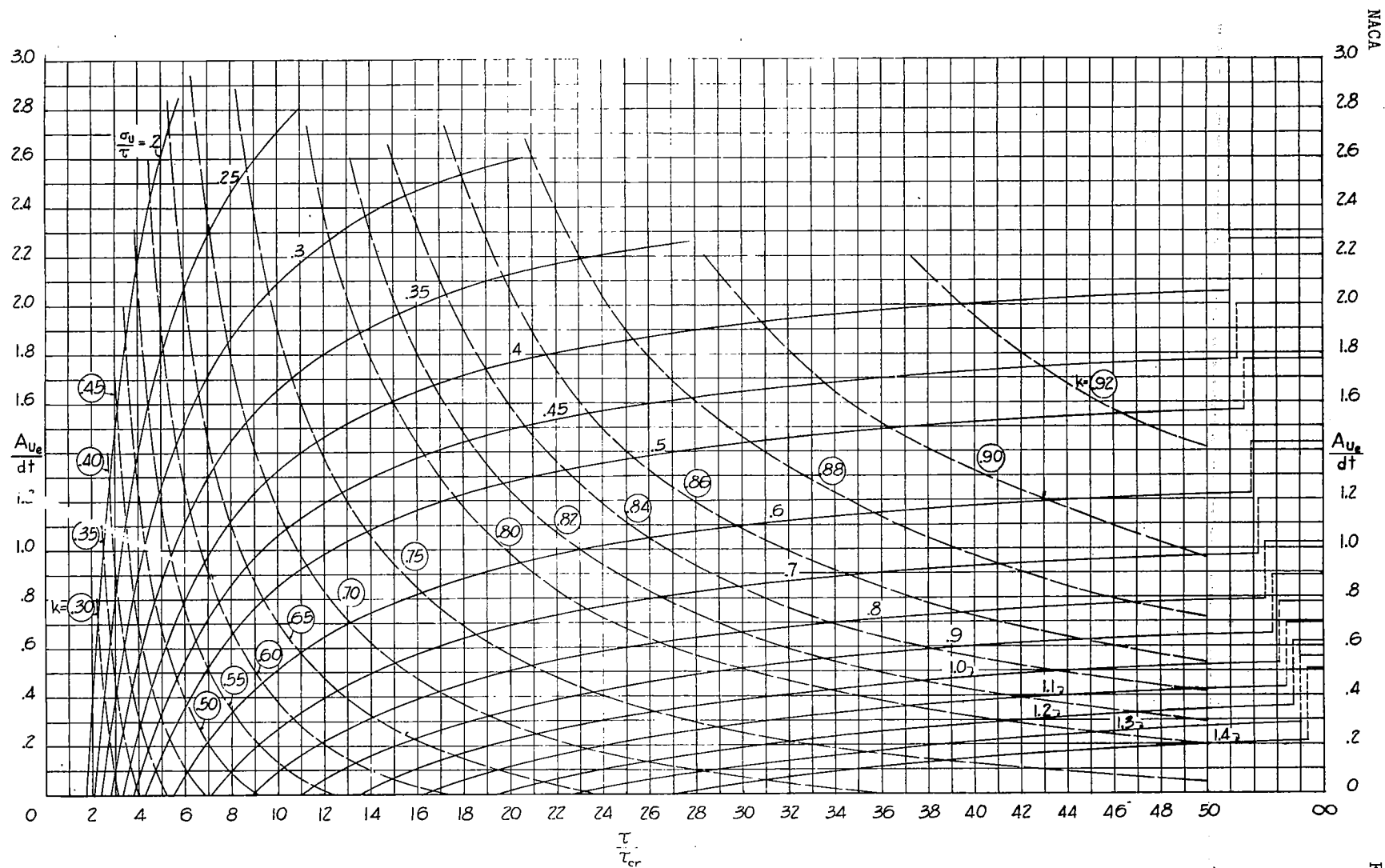


Figure 17.- Design chart 1 for stresses in incomplete diagonal-tension fields.

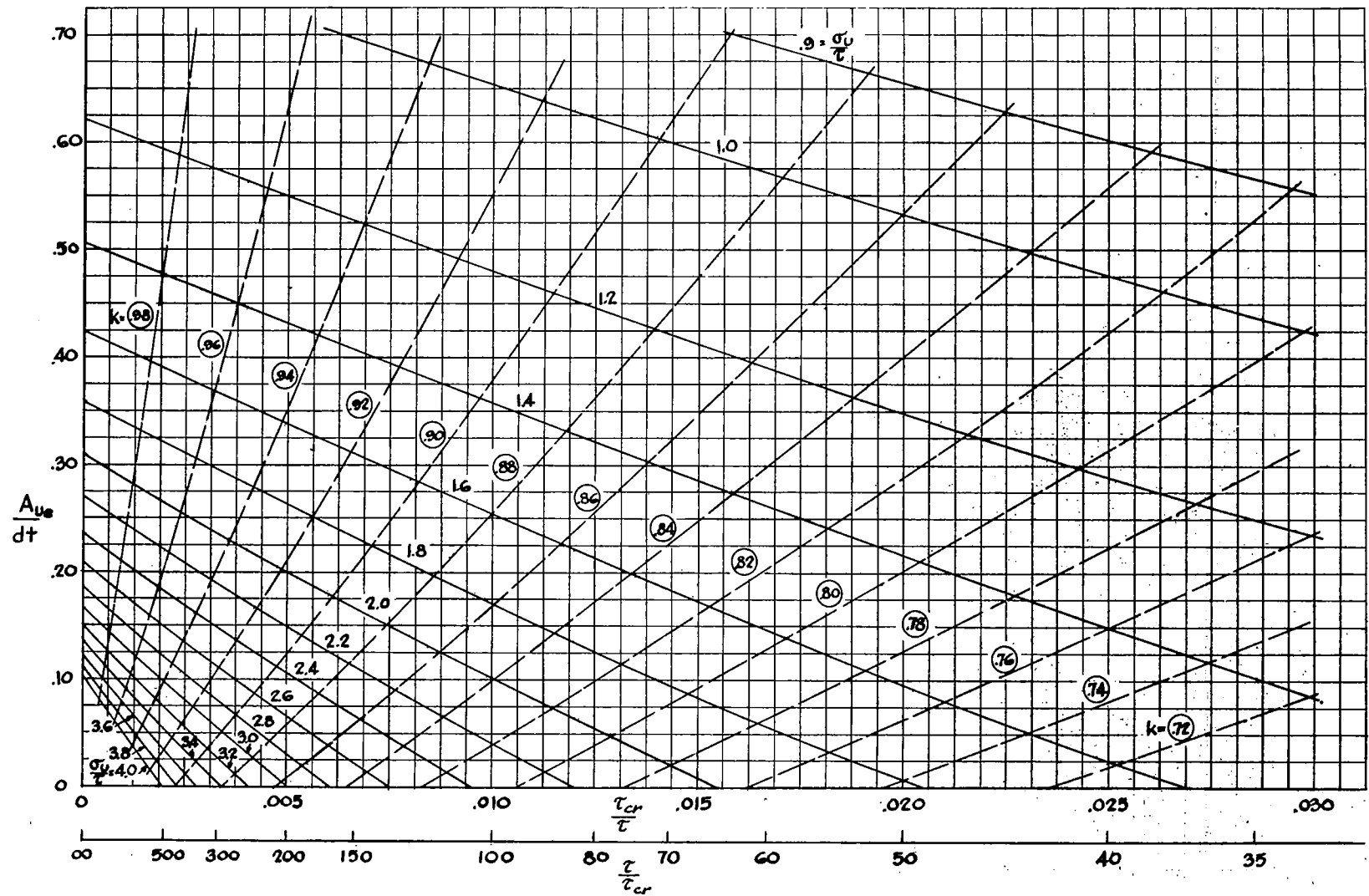


Figure 18.— Design chart 2 for stresses in incomplete diagonal-tension fields.

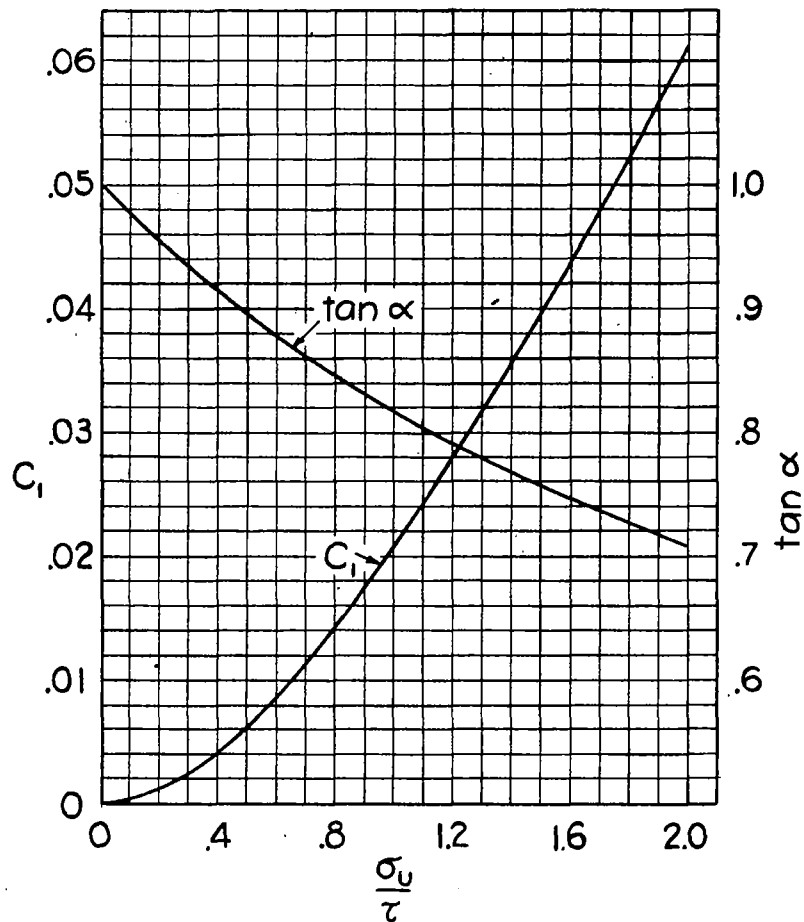


Figure 9.- Stress-concentration factor  $C_1$ .

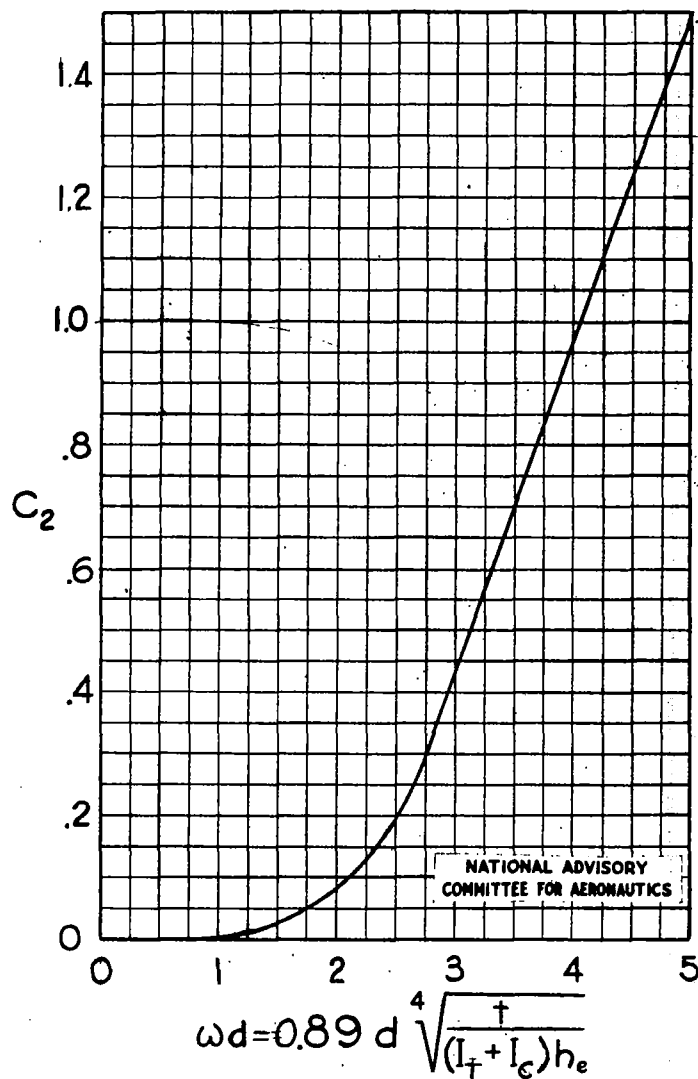
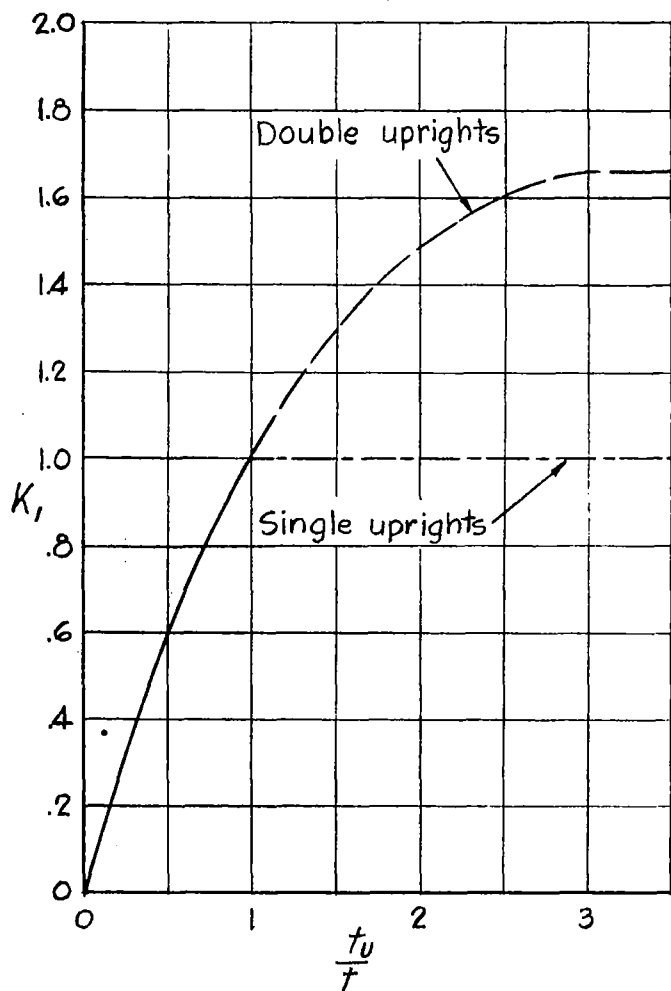
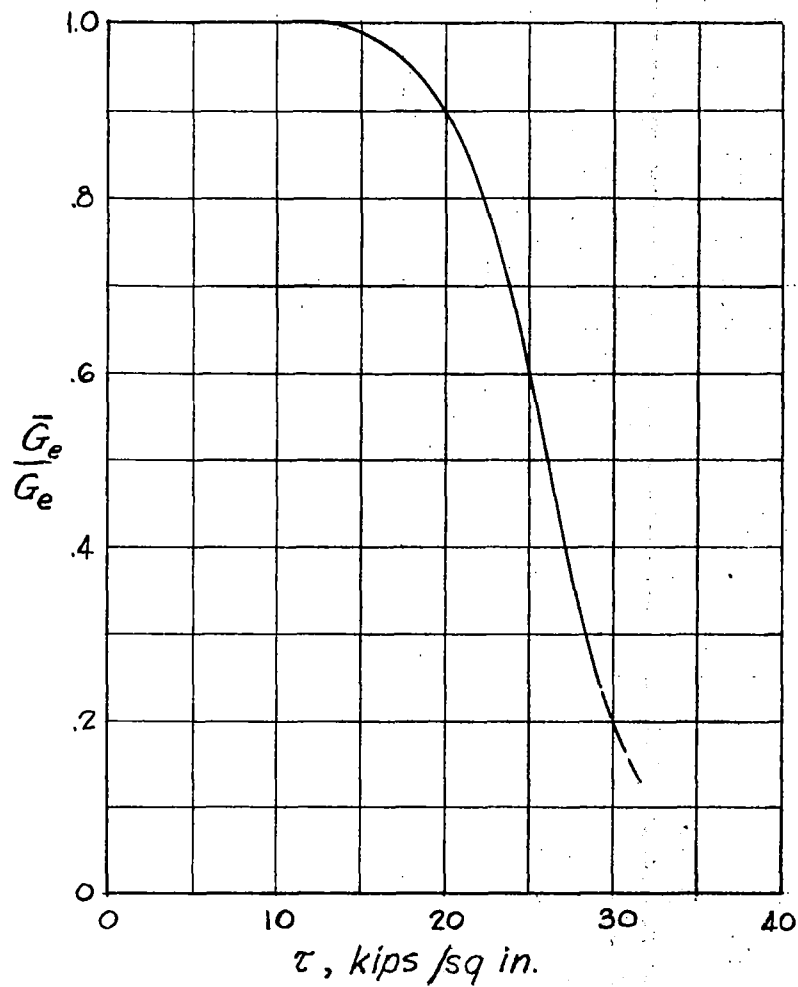


Figure 20.- Stress-concentration factor  $C_2$ .

Figure 25.—Correction factor for  $\tau_{cr}$ .Figure 21.—Tentative curve of  $\bar{G}_e/G_e$  for 24S-T sheet.

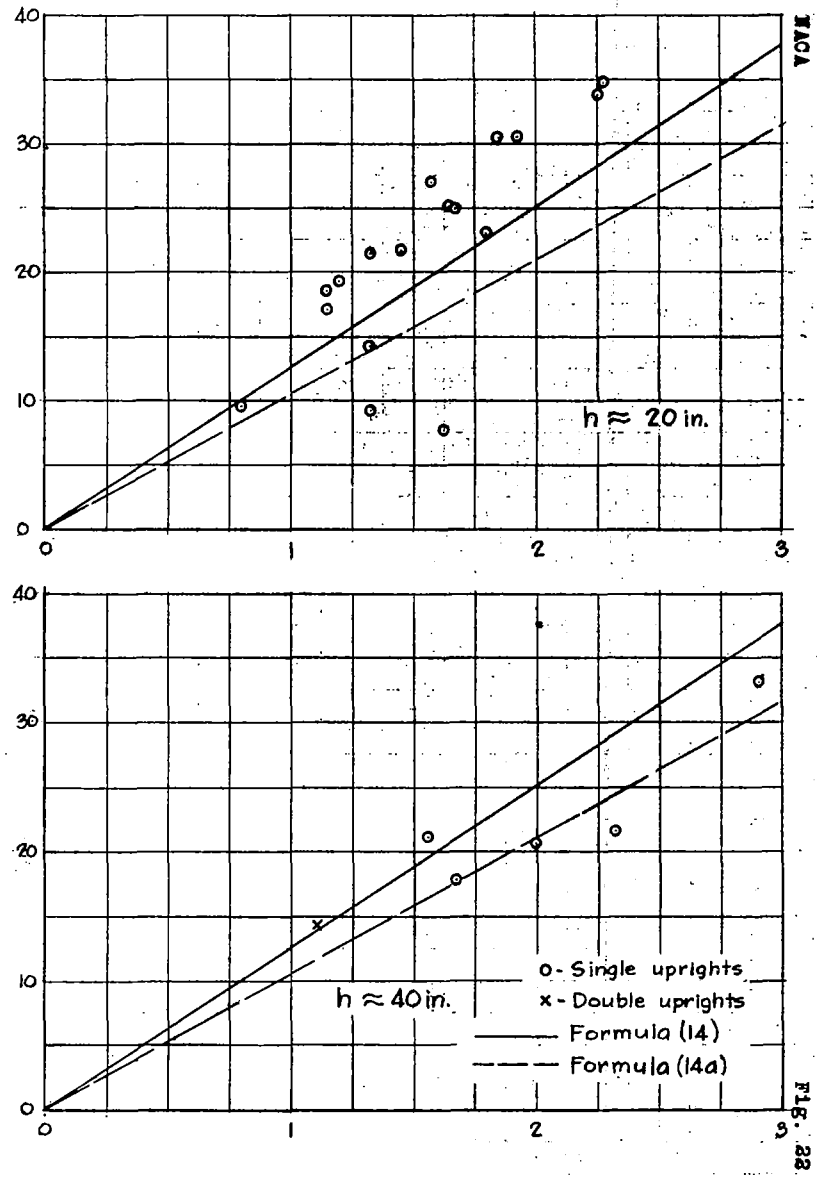
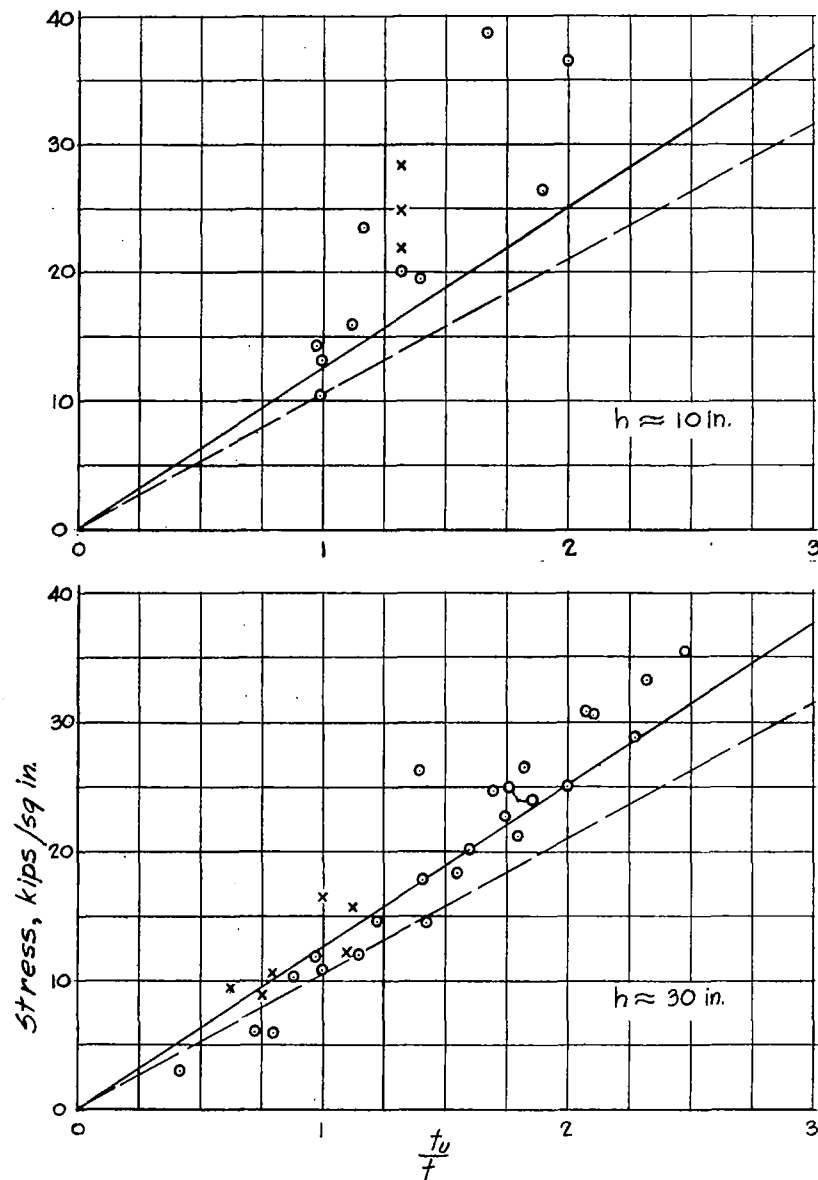


Figure 22.— Stresses in uprights at failure.

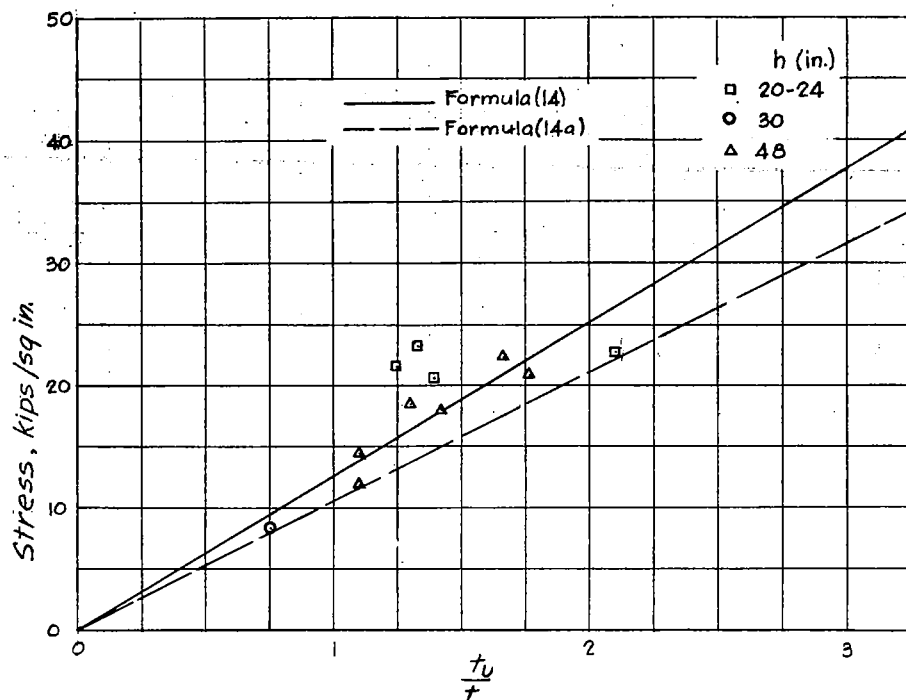


Figure 23.— Stresses in uprights at failure of beams with uprights of alternating size.

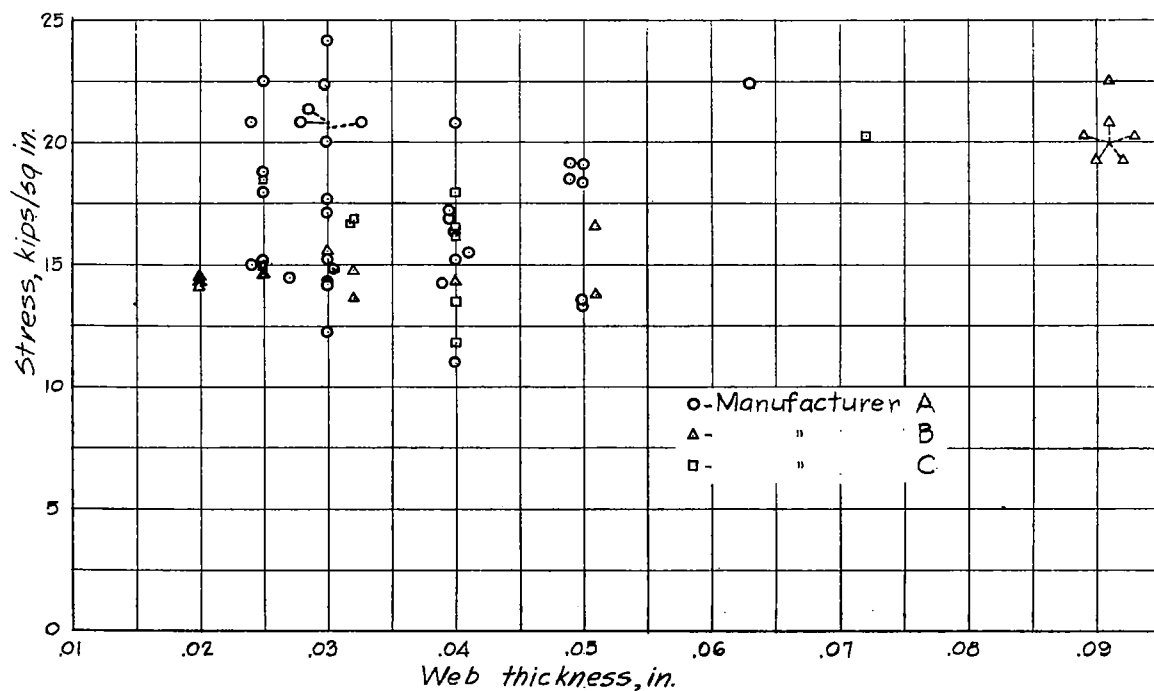


Figure 24.— Shear stresses at yield.

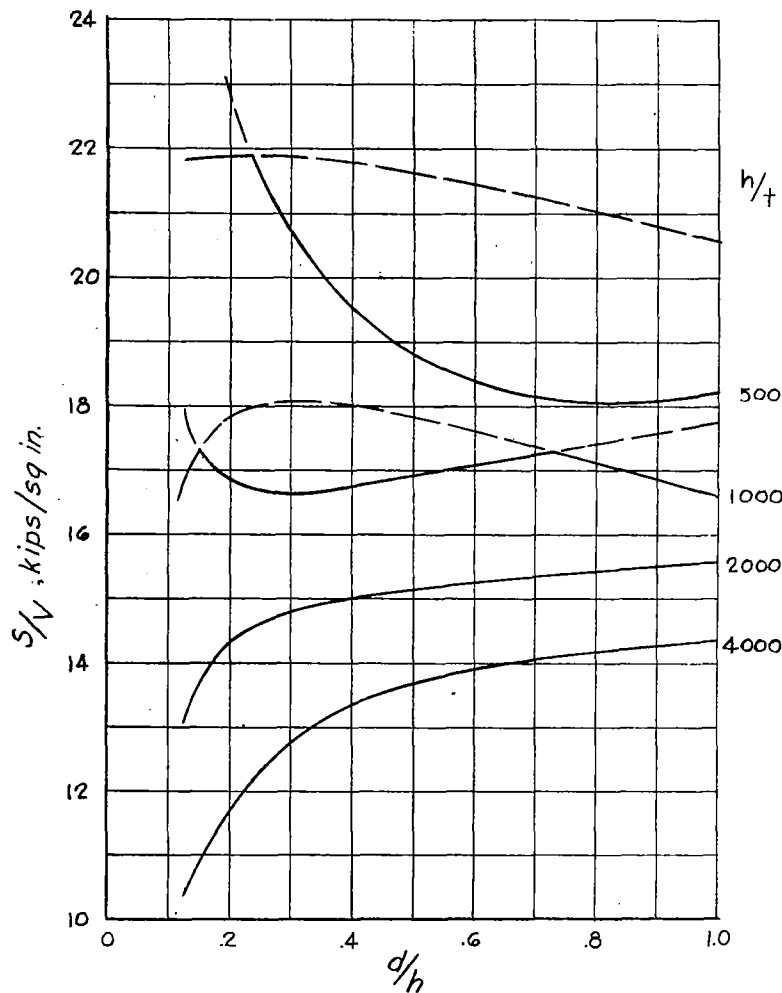


Figure 26.— Strength-volume ratios for diagonal-tension web systems with double uprights.

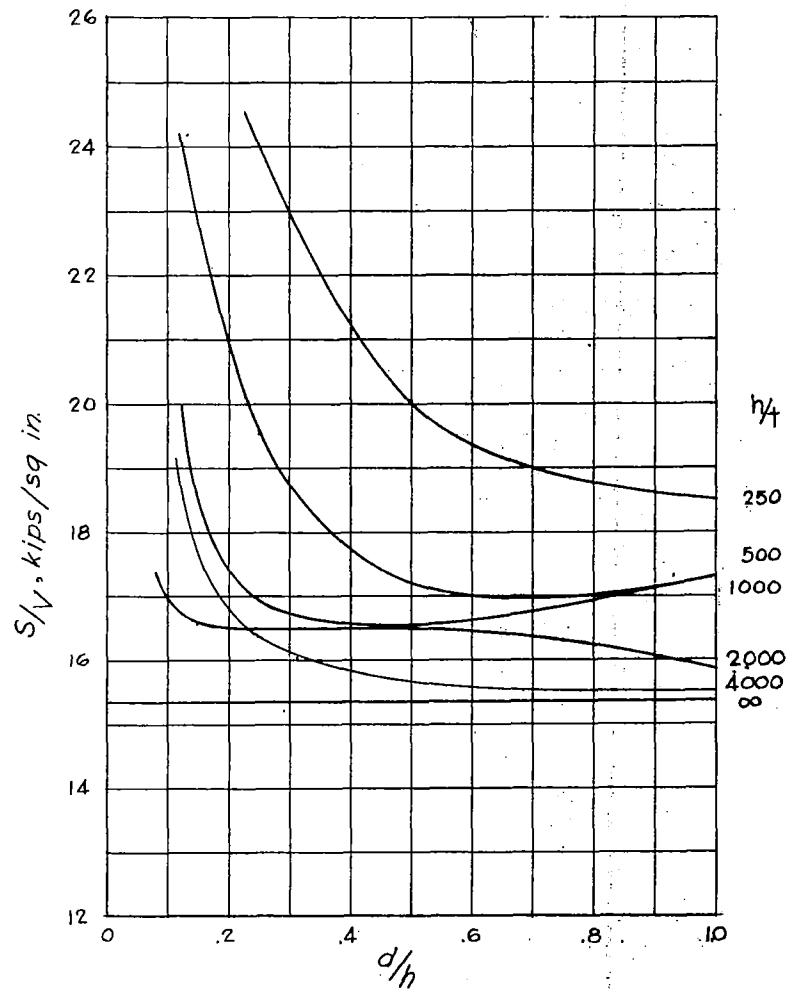


Figure 27.— Strength-volume ratios for diagonal-tension web systems with single uprights.



A-H-B Double uprights failing by bending  
 C-H-D Double uprights failing by twisting  
 E-F-G Single uprights

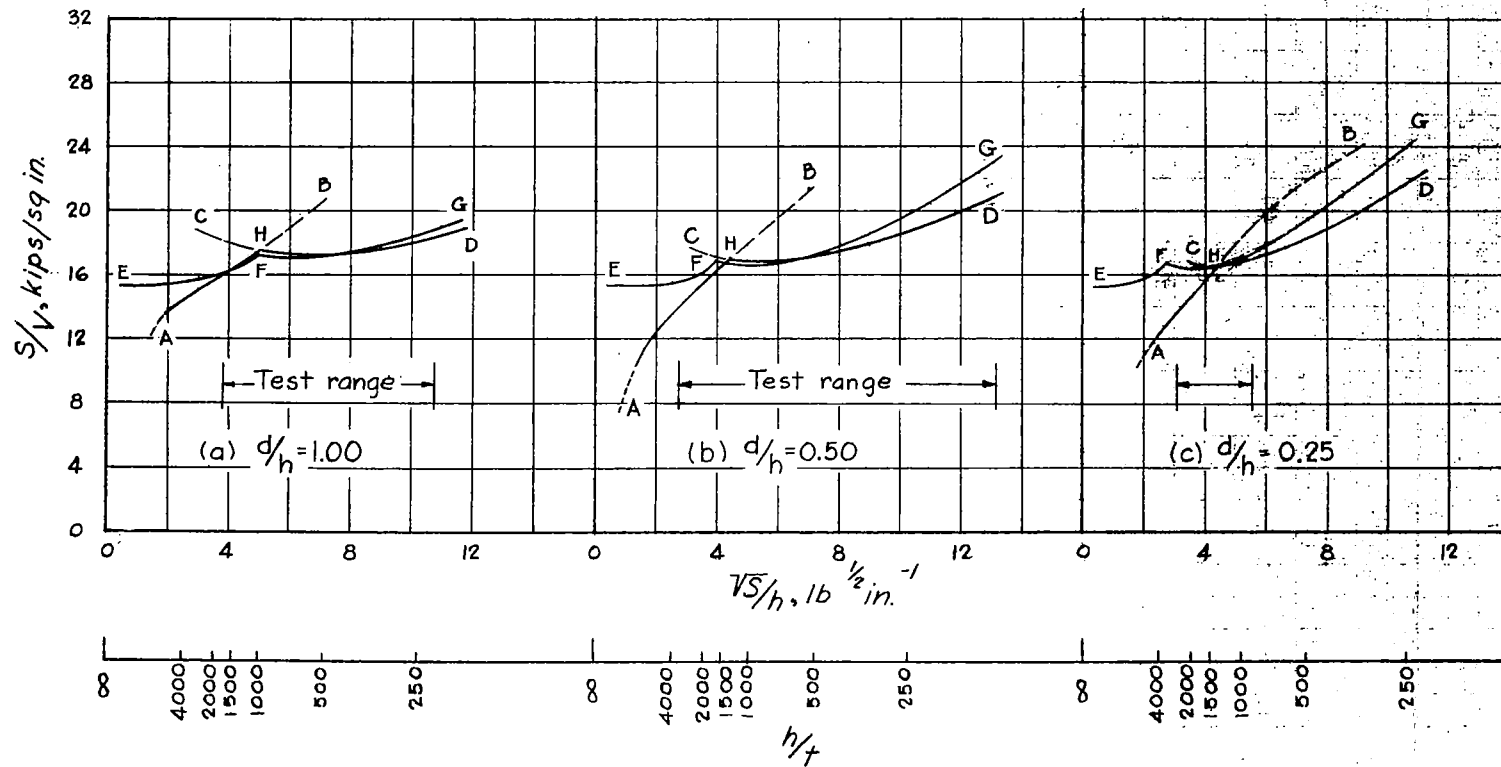
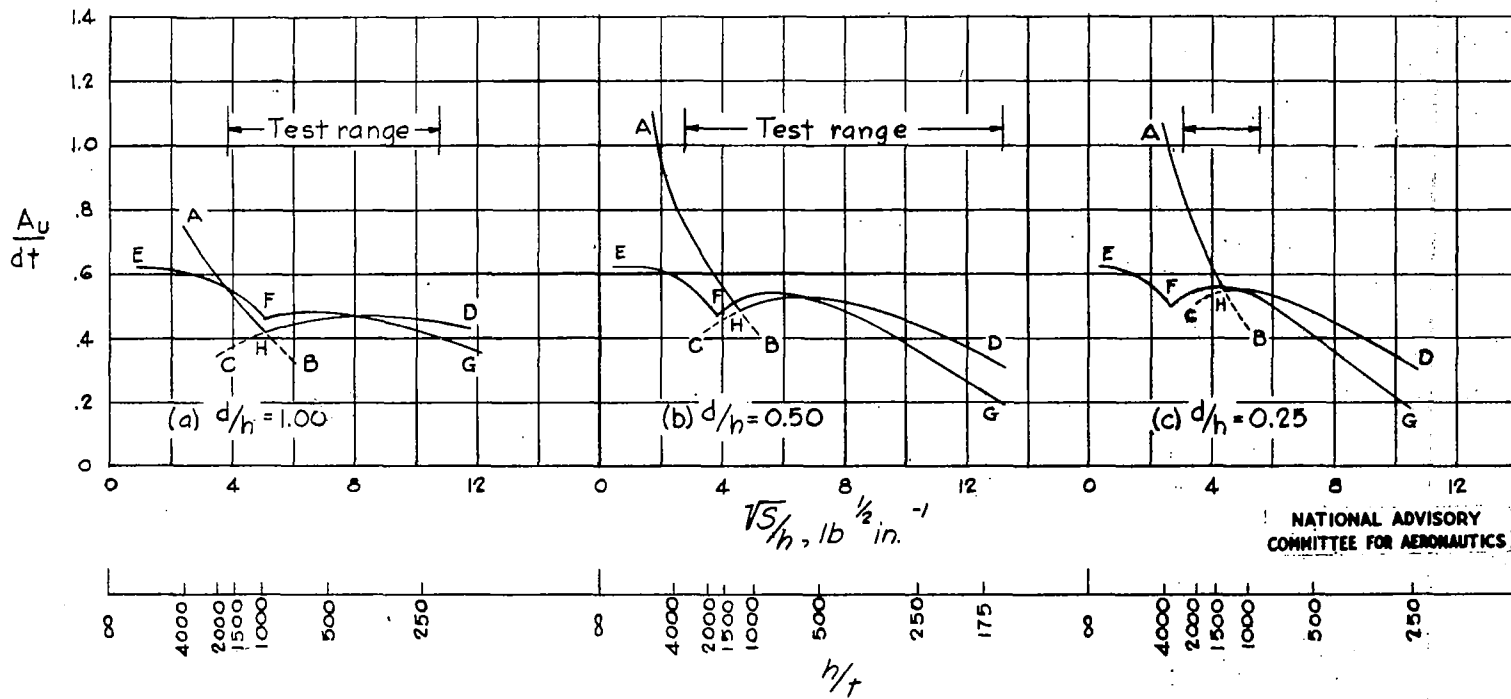


Figure 28.— Strength-volume ratios for diagonal-tension web systems.

A-H-B Double uprights failing by bending  
 C-H-D Double uprights failing by twisting  
 E-F-G Single uprights



NATIONAL ADVISORY  
 COMMITTEE FOR AERONAUTICS

Figure 29.— Reinforcement ratio for diagonal-tension web systems of balanced design.

NASA Technical Library



3 1176 01403 4517